Society of Automotive Engineers, Inc.
400 COMMONWEALTH DRIVE, WARRENDALE, PA. 15096

AEROSPACE RECOMMENDED PRACTICE

ARP 876A

Issued March, 1978
Revised September, 1980

GAS TURBINE JET EXHAUST NOISE PREDICTION

TABLE OF CONTENTS

PREPARED BY:

SAE COMMITTEE A-21, AIRCRAFT NOISE MEASUREMENT

1. INTRODUCTION

AIR 876, issued on 7 October 1965, presented a summary correlation of jet engine exhaust noise data available at that time. It dealt with both static and flight modes, but by virtue of the data largely being from full scale engines, no attempt was made to subdivide the information into the relevant component sources. Work in recent years on good quality noise facilities has established that most engine exhaust systems are influenced in their noise characteristics by far more than the noise due to the external mixing process alone, and this work has provided the opportunity to develop a clearer picture of the influence of other effects.

AIR 876 was also limited to velocities above 1,000ft/sec, i.e. the range of exhaust velocities associated with early jet engines. The introduction of more advanced engine designs demands a prediction technique for exhaust sources over a far wider range of velocity conditions.

Therefore it is intended that ARP 876 be developed on a long term basis as a document definitive in most aspects of the prediction of exhaust noise, consistent with the state of the art, and specific recommended procedures will be issued as Appendices.

The document will offer a method of estimating the exhaust noise from single unsilenced engines. To be useful in estimating the noise from aircraft installations a number of additional effects must be considered, and it is intended that these also will be covered as substantive evidence becomes available.

Areas that will not be addressed, due to source variability with detailed engine design parameters, are aerodynamic blade noise sources; that is the noise generated by interaction effects between rotating and stationary components of the fan, compressor and turbine systems.

Each Appendix will be dated, and will represent an approach to a particular topic as agreed by members of the SAE A-21 Subcommittee with experience or data on that subject. Lists of members and affiliated bodies contributing experimental data or other information as used in compiling any one Appendix will be included. Correspondence should be addressed to the Secretary of the A-21 Committee for appropriate distribution.

2. SOURCES OF EXHAUST NOISE

The exhaust system noise of an aero gas turbine engine can be considered to comprise the following main sources:

a) Pure jet mixing noise resulting from a hot core exhaust stream mixing with its surrounding environment (which may be influenced by a bypass flow).

b) Pure jet mixing noise resulting from a cold bypass stream mixing with both the surrounding environment and the core flow.

c) Shock associated noise, where either or both hot and cold exhaust systems comprise a choked final nozzle.

d) Noise from the core engine resulting from aerodynamic disturbances upstream of or at the final nozzle, including combustion noise.

e) Aerodynamic noise, tonal and broadband, resulting from blade interaction effects in fan, compressor or turbine systems.

All the above sources combine in varying degrees to produce the overall exhaust noise characteristics. The relevance of each source is a function of both engine operating condition and aircraft speed. Because of the dependence of aerodynamic blading noise on the intimate design configuration of any given engine, this aspect is specifically excluded from subsequent condition, and every attempt has been made to remove such phenomena from any engine data used.

3. NOTES ON USE OF PREDICTION PROCEDURES

3.1 Prediction methods contained in this document are self-contained. To develop an estimate of the total exhaust noise signature from an engine it is necessary to integrate the individual source components.

This is effected by estimating each component spectrum and summing the levels in each 1/3 octave logarithmically. This is usually most conveniently carried out prior to any extrapolation to the relevant distance or corrections for atmospheric conditions and ground reflection effects. It is also necessary to incorporate any estimated turbo-machinery content (not covered herein) at the initial stage, in order to obtain a complete engine picture. Furthermore, it is advisable that any assumed modification to the noise by virtue of silencing or installation effects is made in the component calculation stage.

3.2 Methods contained in this document are expressed in terms of noise levels that would be measured under free field conditions. Reflective augmentations and cancellations from real surfaces, primarily the ground surface over which measurements are made, produce peaks and troughs in the observed test spectra, and these have been corrected out of the experimental data used where it has not been obtained under anechoic conditions.

Spectra and directivity plots in this document must, therefore, be converted to non free-field conditions to make them representative of typical measurements "in the field". SAE AIR 1327 provides guidance on such conversion for an acoustically hard surface (i.e. concrete, tarmac) and advice on how to deal with other typical surfaces (e.g. grassland).

3.3 The prediction methods provide spectral information derived from measurements taken in the acoustic far field, but corrected for atmospheric attenuation and normalised.

Since practical distances involved in aircraft noise calculations are large, apart from the normal inverse square law correction, allowance must be made for atmospheric absorption. SAE ARP 866A provides a standard method of allowing for atmospheric absorption under a range of ambient temperatures and humidity conditions.

3.4 If a subjective assessment is required, Perceived Noise Levels (PNL) may be calculated using the methods in SAE ARP 865A.

3.5 Prediction methods are directed at producing estimates of noise levels generated during the normal take-off and approach regimes of aircraft operation. Extrapolation of the methods to higher flight speeds, or use for estimation other than in the acoustic farfield, is not recommended since experimental evidence in support of such extrapolation is not available.

4. SYMBOLS

a_o	Ambient speed of sound	m/s
A_j	Cross-sectional area of jet exhaust nozzle	m^2
C_v	Velocity coefficient for relevant discharge nozzle	
dB	Sound Pressure Level (re 20 Micro Pa.)	dB
D_j	Exhaust nozzle diameter	m

4. (Continued)

	f	One-third octave centre band frequency	Hz
	g	Gravitational constant	m/s^2
	ISA	International Standard Atmosphere	
Ø	$m(\theta_i)$	Relative Velocity exponent used in converting static mixing noise to flight conditions	
Ø	M_a	Aircraft flight Mach. Numbers $\left(\frac{V_a}{a_o}\right)$	
	NPR	Nozzle pressure ratio	
	OASPL	Overall Sound Pressure Level	dB
	P_o	Ambient pressure	Pa
	P_{ISA}	Ambient pressure under ISA conditions	Pa
	r	Radial distance from nozzle exit to observer	m
	R	Gas constant with value 287.05 J/kg°K based on the universal gas constant of 8.31432 J/mole°K and mass per mole in dry air of 28.9644×10^{-3}kg/mole	J/kg°K
	S	Normalised Free-Field Overall Sound Pressure Level	dB
	SPL	Sound Pressure Level	dB
	T_j	Jet Total Temperature	K
	V_a	Forward speed of engine/airplane	m/s
	V_j	Fully expanded jet velocity	m/s
	γ	Ratio of specific heats for propulsive medium	
	θ_i	Angle to engine inlet axis	degrees
	θ_j	Angle to engine jet axis ($180° - \theta_i$)	degrees
	ρ_{ISA}	Atmospheric density under ISA conditions (1.225 kg/m^3 based on atmospheric pressure of 1.01325×10^5 N/m^2 at an air temperature of 288.15°K)	kg/m^3
	ρ_j	Fully expanded jet density	kg/m^3
	ω	Variable density index used in computing jet mixing noise OASPL	
Ø	ϕ	Angle between direction of aircraft motion and direction of sound propagation	degrees
	ξ	Strouhal frequency correction factor	

NOTE: The units quoted above for the physical quantities are the recommended System Internationale units. Except for the logarithmic quantities, temperatures and angles, any other consistent system of units may be used since results are expressed as dimensionless ratios.

APPENDIX A

DATE OF COMPILATION
Static Conditions - September 1976
Flight Conditions - November 1978

5. PREDICTION OF SINGLE STREAM JET MIXING NOISE FROM SHOCK FREE CIRCULAR NOZZLES

5.1 Static Conditions: Definitive model scale experimental work of recent years has provided a firm data base for the study of mixing noise over a wide range of jet velocity and temperature conditions. This work has shown that jet mixing noise level and Spectral Character is a function of the following principal parameters:

a) The velocity differential between the jet and its environment.

b) The jet density relative to its environment.

c) The jet dimensions.

It has been concluded that one of the most convenient ways to express jet noise characteristics is to consider firstly the normalized overall sound pressure level (OASPL) as a function of jet velocity (V_j) and angle of measurement (θ_i or θ_j) and to then relate the spectral character (on one-third octave basis) to the overall level at any point in the field. This procedure may be adopted by using Figs. A.1 through A.11. The information of Fig. A.1 through Fig. A.11 is also presented in tables A.1 through A.11.

The method of calculation is as follows:

Step 1 - Calculate the Fully Expanded Mean Jet Velocity (V_j) from a knowledge of jet temperature and pressure, where:

$$V_j = C_v \left[\left(\frac{2\gamma R}{\gamma - 1} \right) T_j \left\{ 1 - NPR^{-\left(\frac{\gamma - 1}{\gamma} \right)} \right\} \right]^{1/2}$$

or, where a knowledge of temperature and pressure is not readily available (for example, from engine test stand measurements) an alternative method of calculating V_j is from thrust and mass flow, where:

$$V_j = \left\{ \frac{\text{Static Gross Thrust}}{\text{Mass Flow}} \right\}$$

Step 2 - Using V_j obtained from Step 1 and the Ambient Speed of Sound (a_o) obtain the Variable Density Index (ω) from Fig. A.1.

Step 3 - For any desired angle and jet velocity use Fig. A.2 to obtain the free-field Overall Sound Pressure Level (S) where:

$$S = OASPL - 10 \log_{10} \left\{ \left(\frac{\rho_j}{\rho_o} \right)^{\omega} \left(\frac{A_j}{r^2} \right) \right\} - 20 \log_{10} \left(\frac{P_o}{P_{ISA}} \right)$$

for the value of V_j at any desired angle.

5.1 (Continued)

Step 4 - Calculate the Overall Sound Pressure Level (OASPL) where:

$$OASPL = S + 10\log_{10}\left(\frac{\rho_j}{\rho_o}\right)^{\omega} + 10\log_{10}\left(\frac{A_j}{r^2}\right) + 20\log_{10}\left(\frac{P_o}{P_{ISA}}\right)$$

Step 5 - Calculate the one third octave band spectral levels from Fig. A.3 - A.11 using jet velocity (V_j), temperature ratio $\left[\frac{T_j}{T_o}\right]$, nozzle diameter

(D_j) and the angle (θ_i) as follows:

Determine ξ from Fig. A.3 and then calculate $\left[\frac{f\ D_j}{V_j} \times \frac{1}{\xi}\right]$ for each 1/3 octave band centre frequency. Enter Figures A.4 to A.11 with the values of $\left[\frac{f\ D_j}{V_j}\ \frac{1}{\xi}\right]$, and values of $\left(\frac{T_j}{T_o}\right)$, $\log_{10}\left(\frac{V_j}{a_o}\right)$ and θ_i to determine values of

1/3 octave band (SPL - OASPL).

For values other than specified in Figures A.3 - A.11, linear interpolation on angles (θ_i), $\log_{10}\left[\frac{f\ D_j}{V_j} \times \frac{1}{\xi}\right]$, $\log_{10}\left(\frac{V_j}{a_o}\right)$ and $\left(\frac{T_j}{T_o}\right)$ is recommended.

5.1 (Continued)

Step 6 - From value of OASPL and 1/3 octave band (SPL - OASPL) as derived in steps 4 and 5 respectively, calculate values of 1/3 octave band SPL.

These values represent the free-field jet noise spectrum at position (r, θ_i) in loss free atmosphere.

Note 1 The spectra of Figures A.3 - A.11 satisfy the following condition

$$\log_{10}\left\{\sum_{i=1}^{N} 10^{\frac{(SPL - OASPL)i}{10}}\right\} = 0$$

Over the range of 1/3 octave frequencies defined by

$$-1.6 \leqslant \log_{10}\left[\frac{f\,D}{\xi\,V_j}\right] \leqslant 1.6$$

Note 2 Accuracy of Prediction

The accuracy of prediction of OASPL at $(r_1\ \theta_1)$ relative to the model data on which it is based varies between $\pm$ 2dB at low jet velocities to $\pm$ 4dB at very high jet velocities. The accuracy of prediction of 1/3 octave (SPL - OASPL) varies between $\pm$ 1dB at peak noise frequencies. However, these limits apply to the extreme cases. For all normal purposes, the majority of predictions will be accurate within $\pm$ 3dB at all frequencies.

Note 3 For the derivation and substantiation of the method, reference may be made to the following documents:

(i) Boeing Document No. D6 - 42929 -1 Empirical Jet Noise Predictions for Single and Dual Flow Jets and without Suppressor Nozzles Volume 1. Single flow Subsonic and Supersonic Jets. C. L. Jeack, S. J. Cowan, R. P. Gerend.

(ii) SNECMA Document YKA No. 5898/76 Comparison des spectres 1/3 d'octave de bruit de jet mesures en chambre sourde A 17 de CEPr aux diverses propositions de revision de l'ARP 876 de la SAE.

(iii) SNECMA Document YKA No. 5317/75 Revision de la methode de prevision du bruit des jets (SAE ARP 876).

Variable density index ω

FIG. AI.

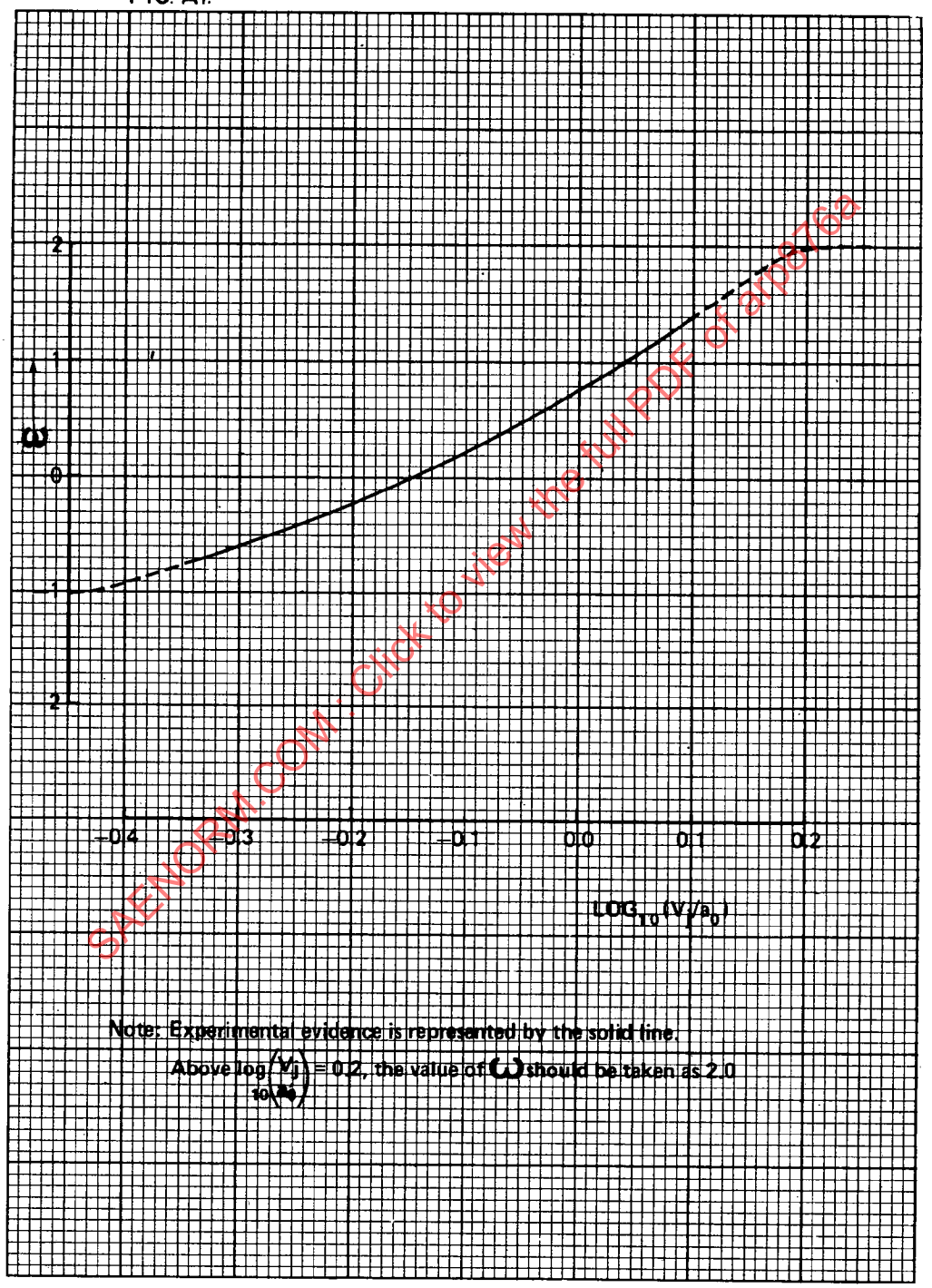

Note: Experimental evidence is represented by the solid line.

Above $\log(V_j) = 0.2$, the value of ω should be taken as 2.0

FIG. A2.

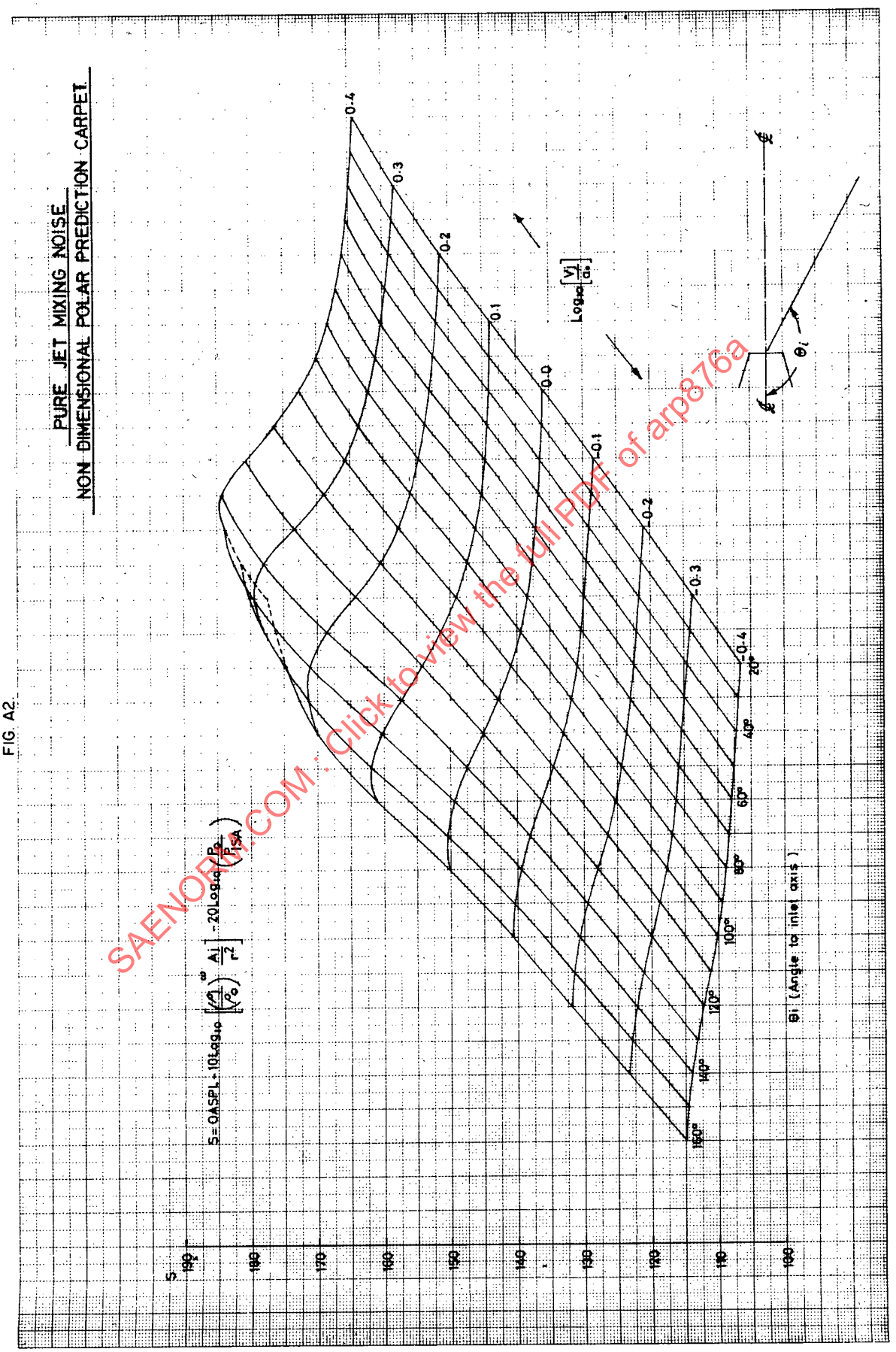

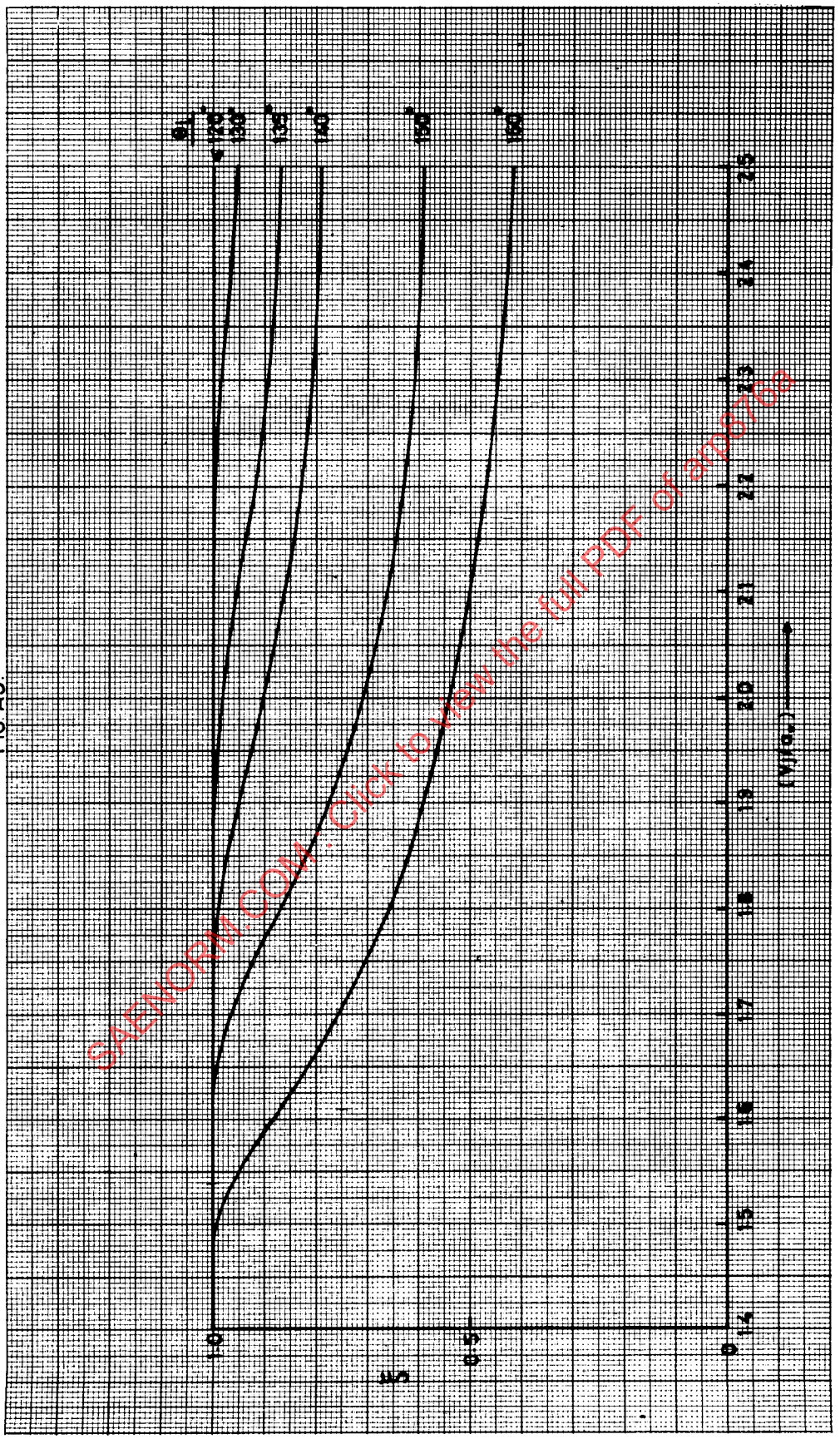

FIG. A3.

FIG. A4.

1/3 OCTAVE BAND NORMALISED SPECTRA. $\theta_i \leq 90°$

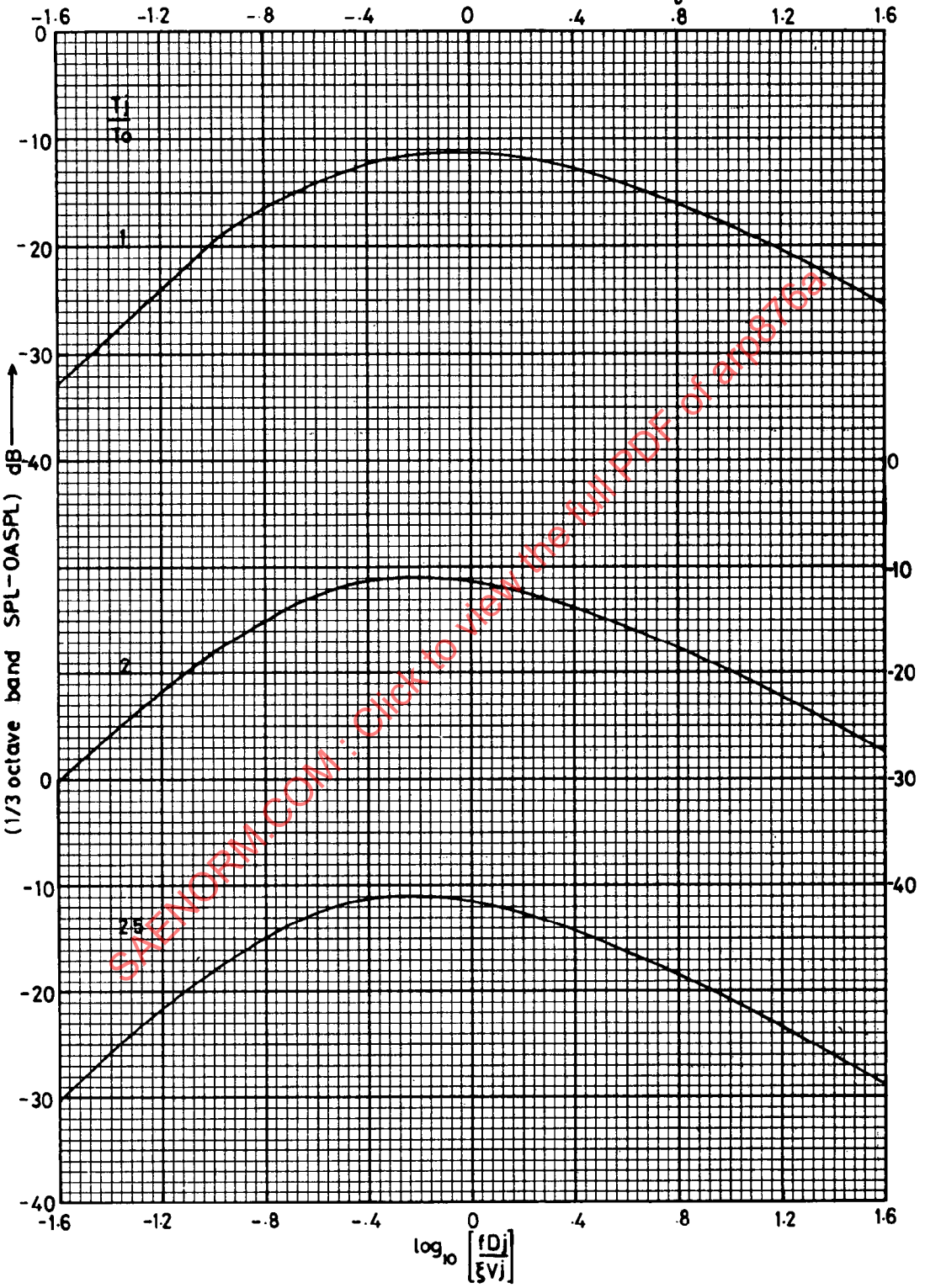

FIG. A4. (CONT'D)
1/3 OCTAVE BAND NORMALISED SPECTRA. $\theta_i \leq 90°$

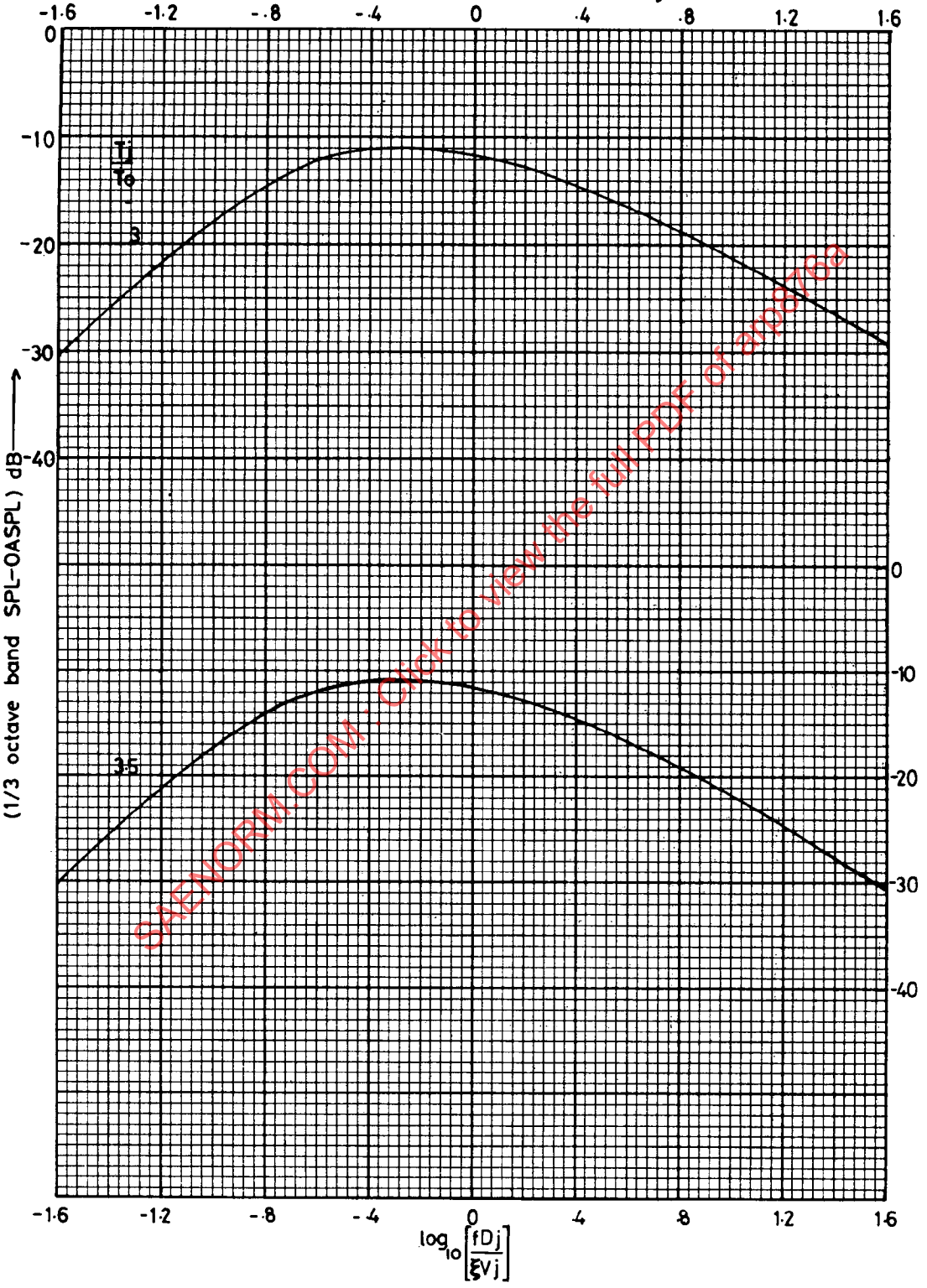

FIG. A5.
1/3 OCTAVE BAND NORMALISED SPECTRA. $\theta_i = 100°$

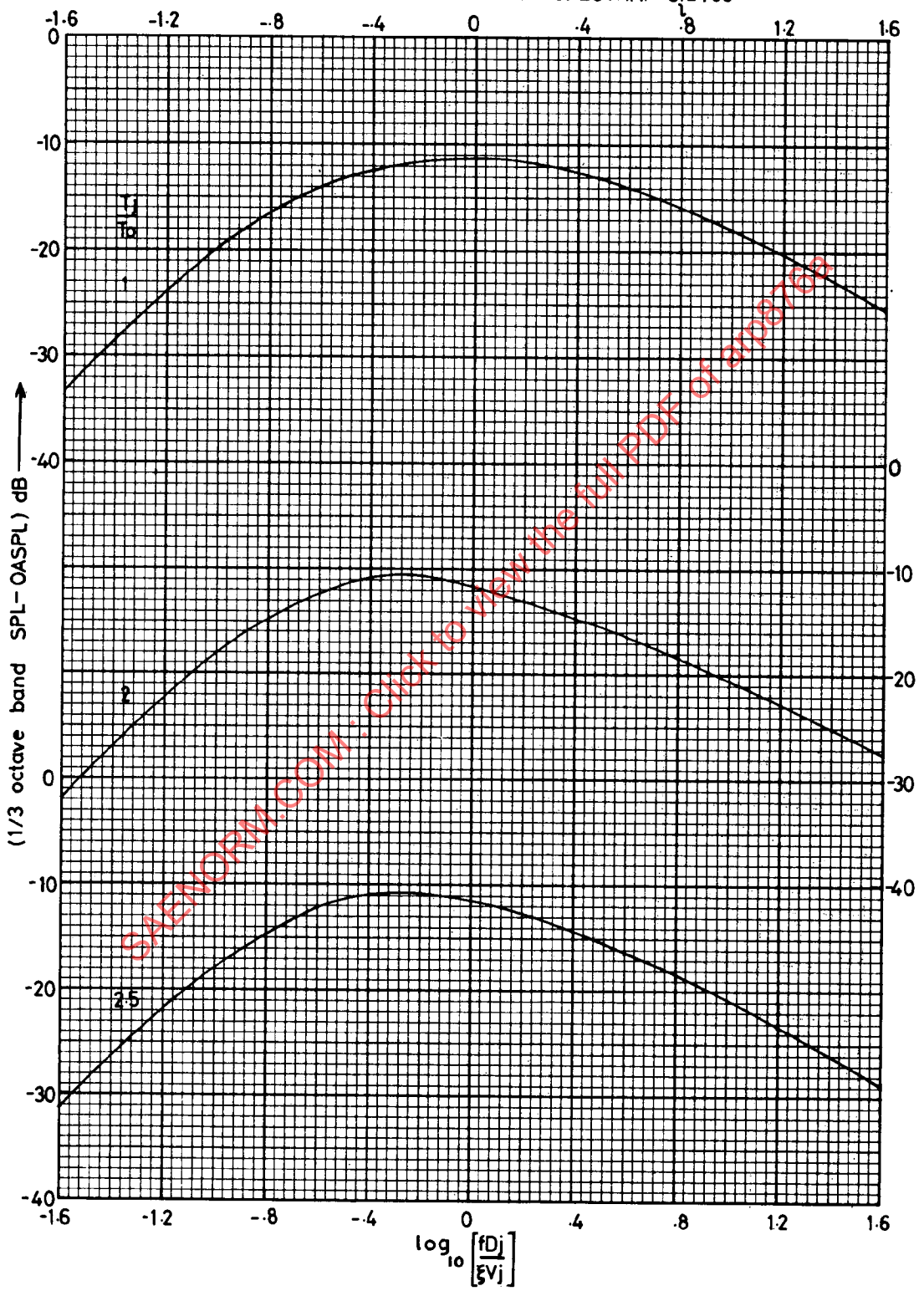

FIG. A5. (CONT'D)

1/3 OCTAVE BAND NORMALISED SPECTRA. $\theta_i = 100°$

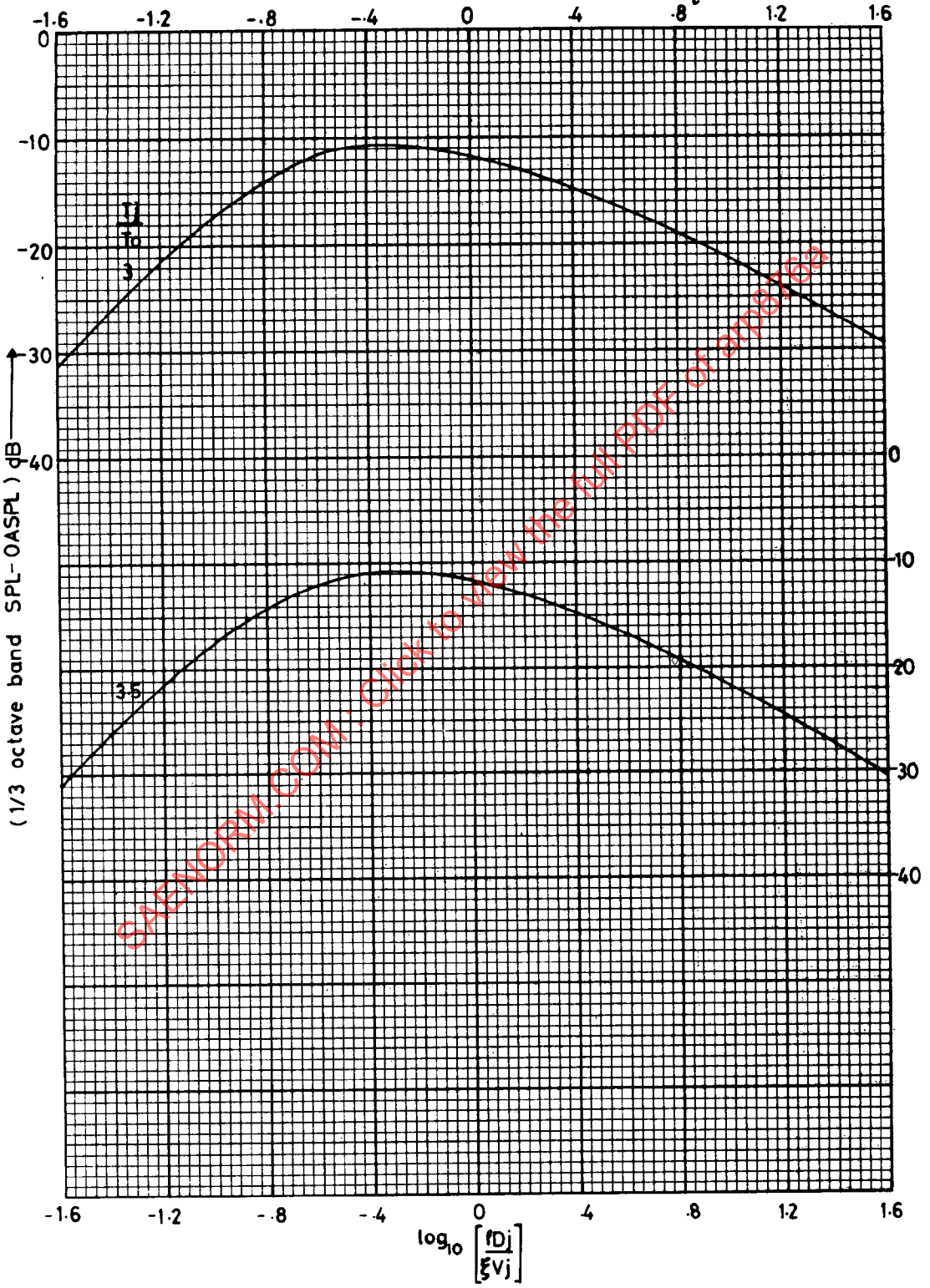

FIG. A6.

1/3 OCTAVE BAND NORMALISED SPECTRA. $\theta_i = 110°$

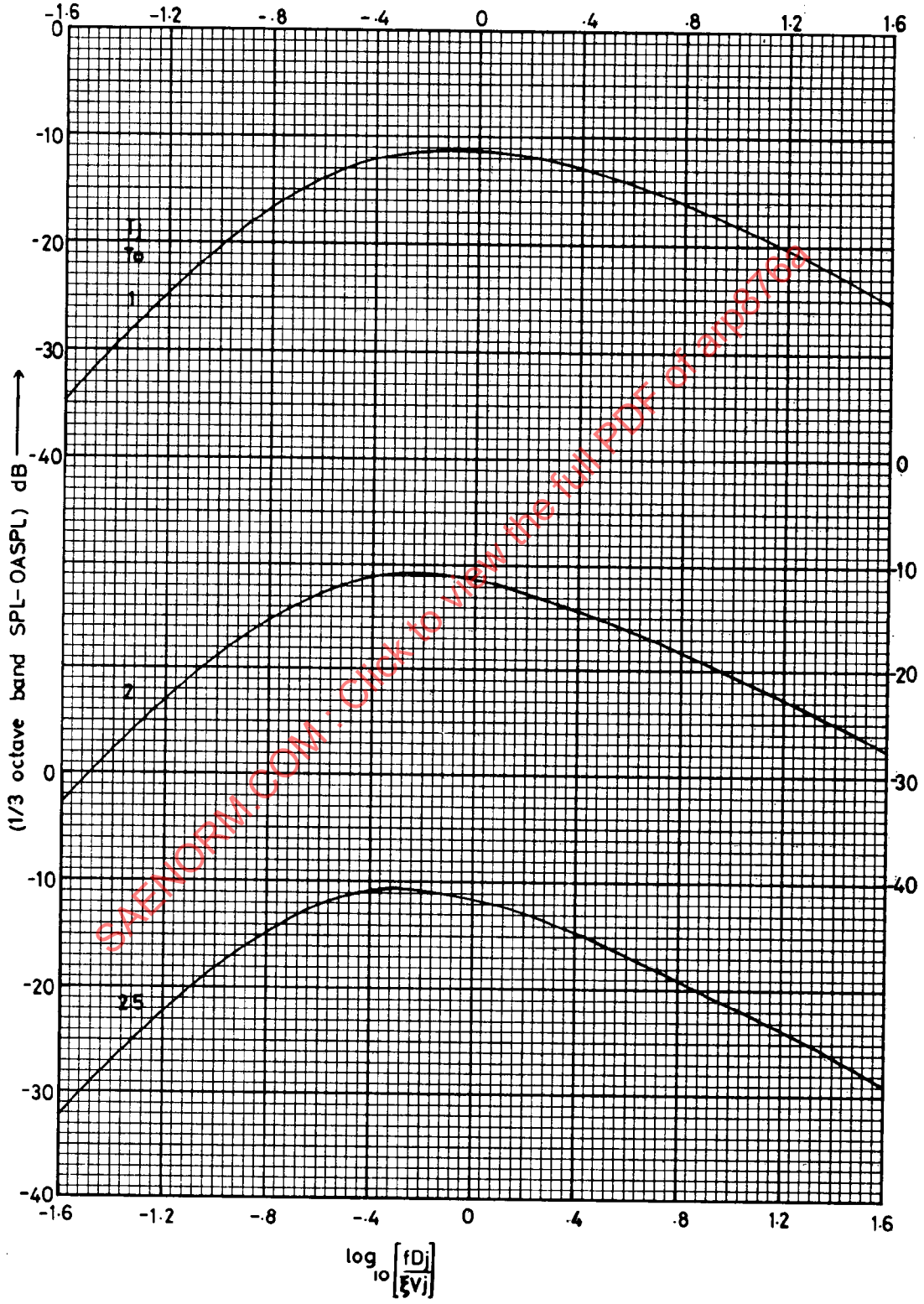

FIG. A6. (CONT'D)

1/3 OCTAVE BAND NORMALISED SPECTRA. $\theta_i = 110^\circ$

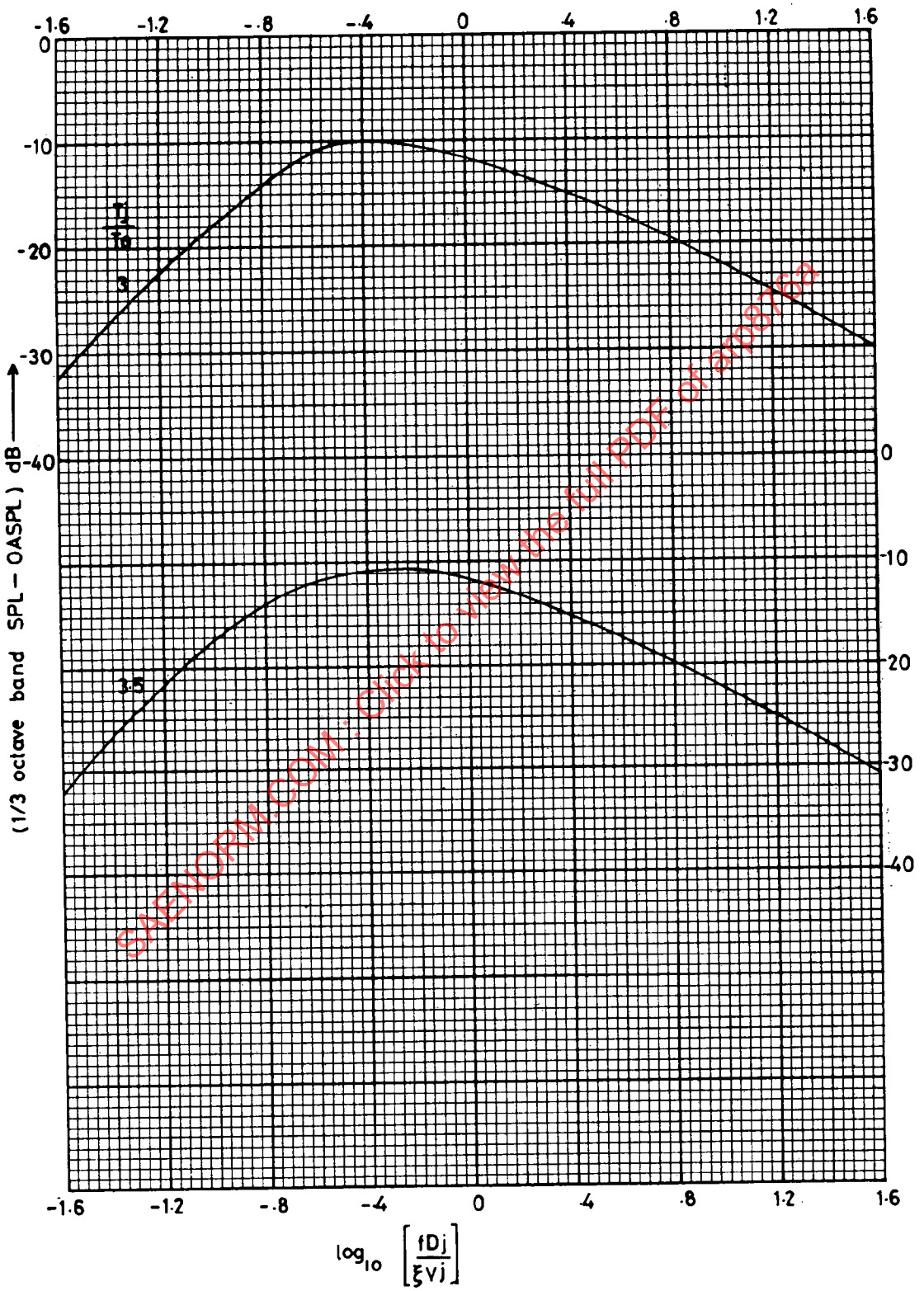

FIG. A7.

1/3 OCTAVE BAND NORMALISED SPECTRA. $\theta_i = 120°$

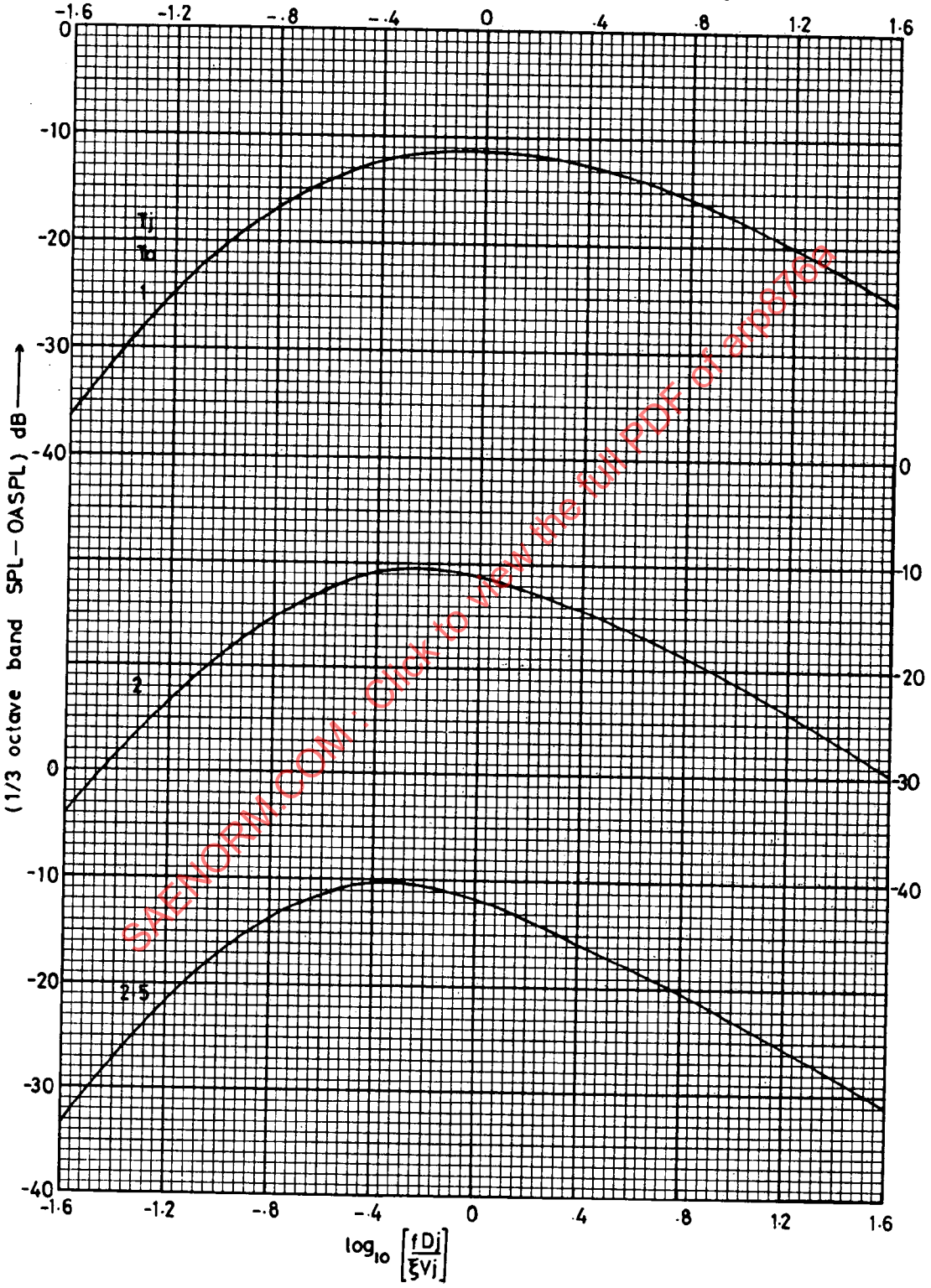

FIG. A7. (CONT'D)

1/3 OCTAVE BAND NORMALISED SPECTRA. $\theta_i = 120°$

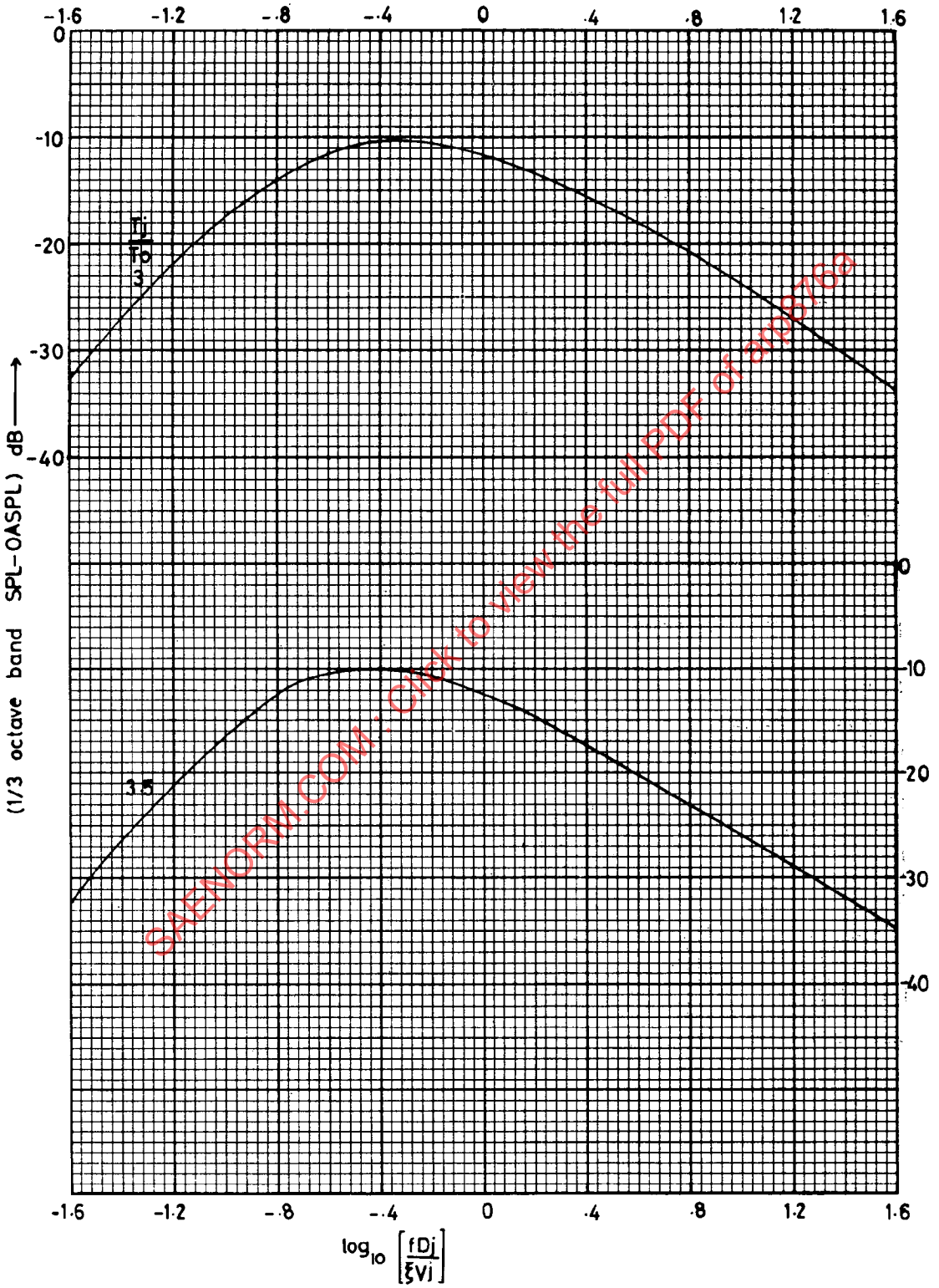

FIG. A8.

1/3 OCTAVE BAND NORMALISED SPECTRA. $\theta_i = 130°$.

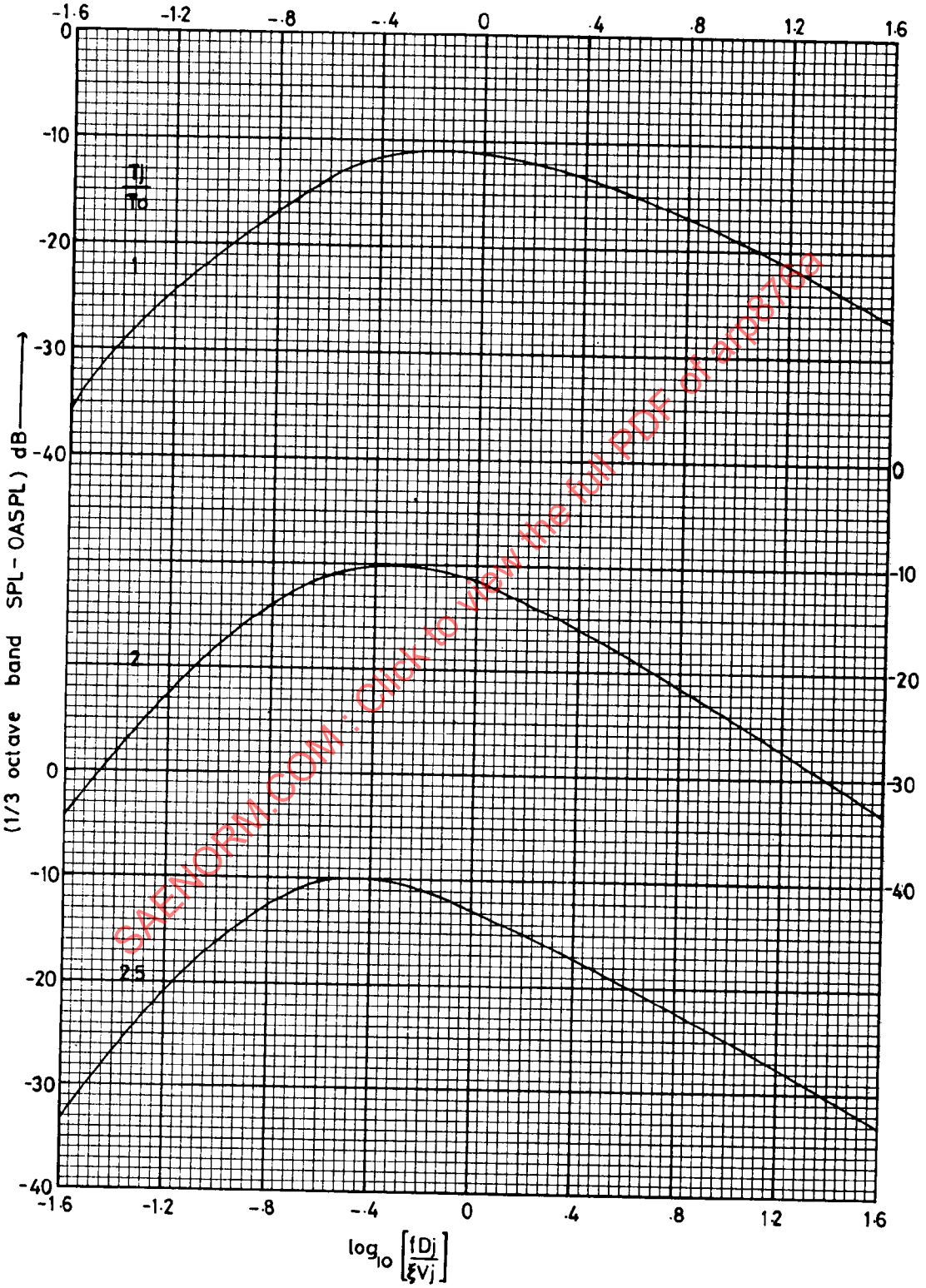

FIG. A8. (CONT'D)

1/3 OCTAVE BAND NORMALISED SPECTRA. $\theta_i = 130°$

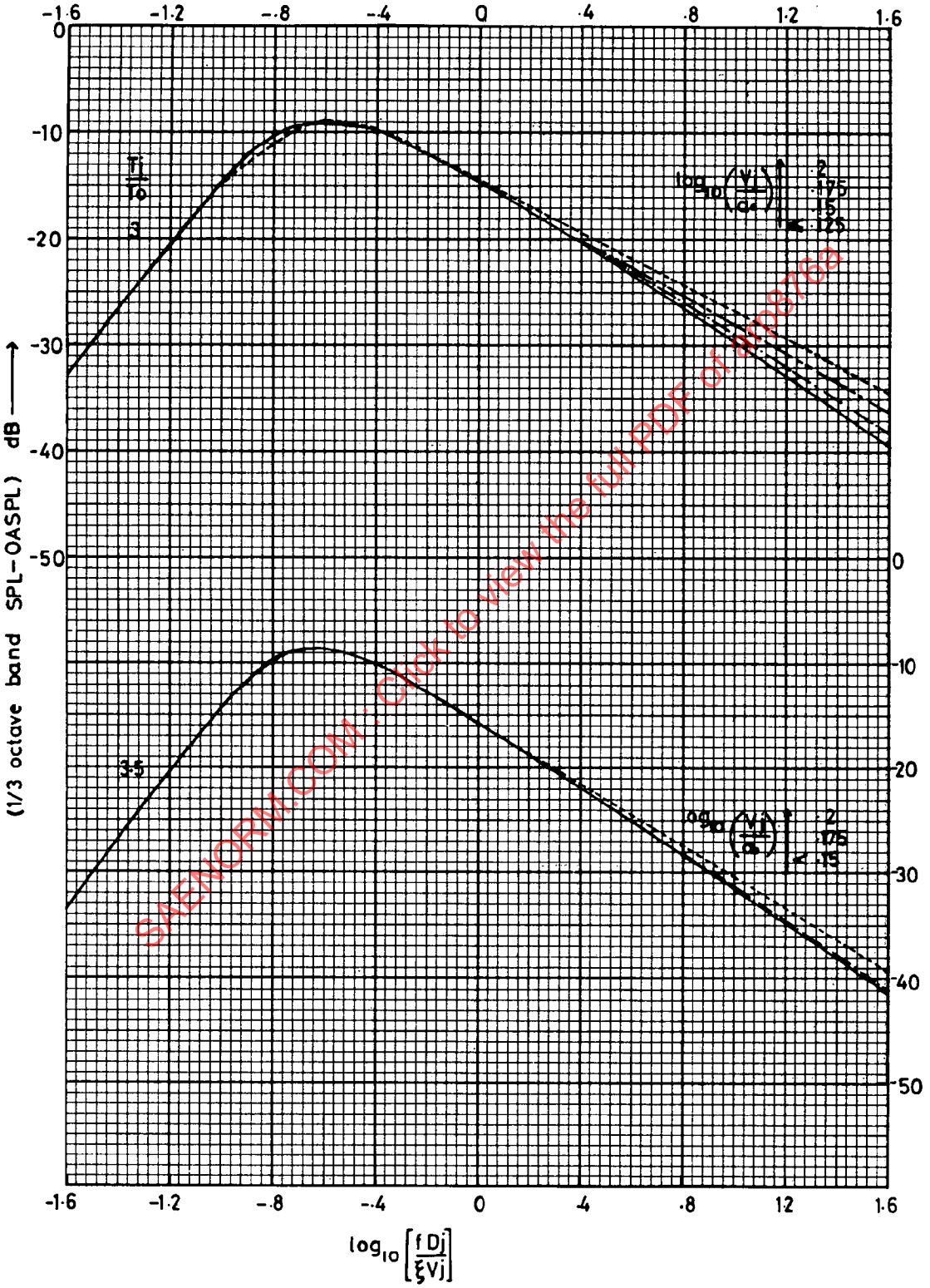

FIG. A9.

1/3 OCTAVE BAND NORMALISED SPECTRA. $\theta_i = 140^\circ$

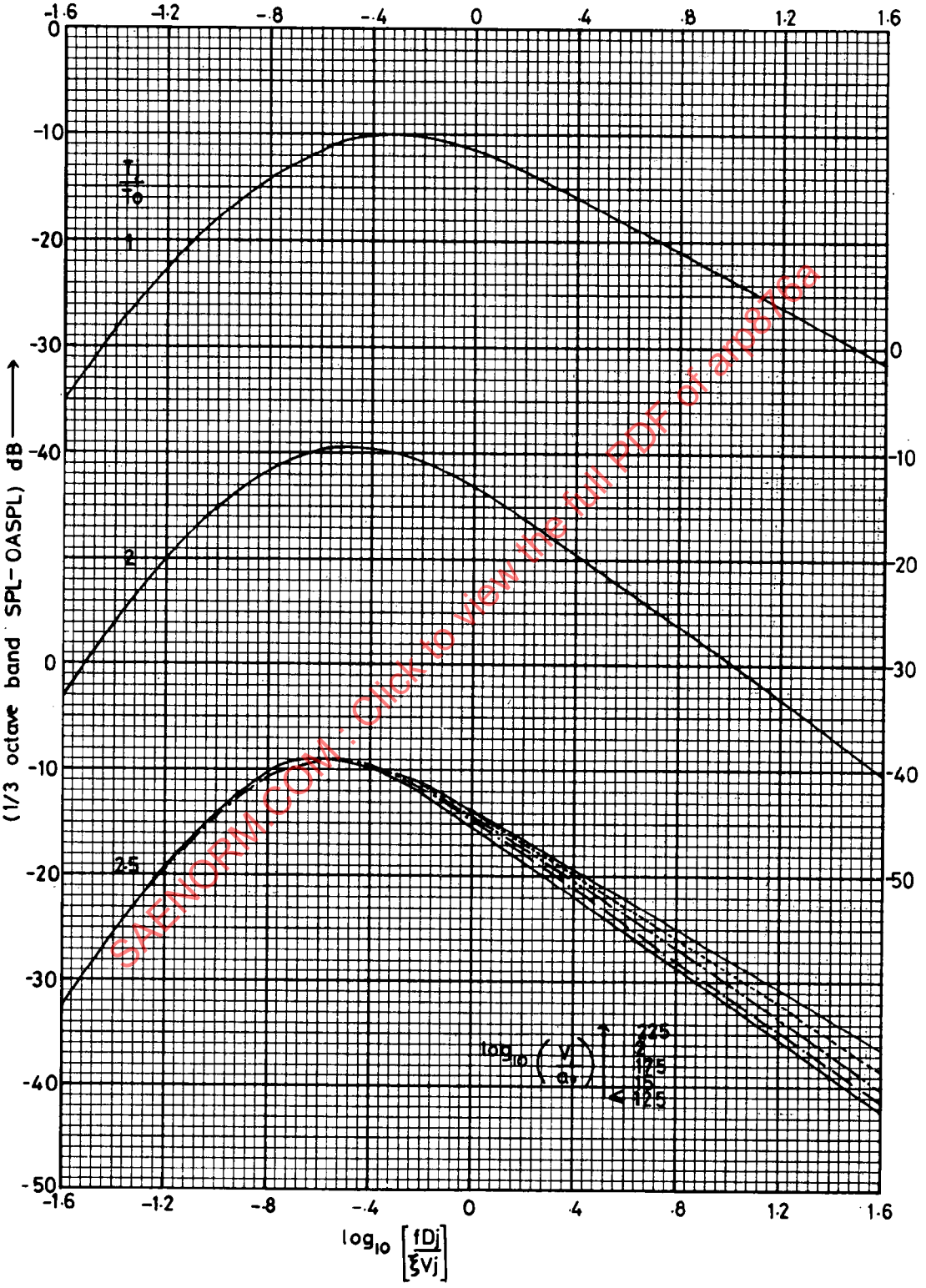

FIG. A9. (CONT'D)

1/3 OCTAVE BAND NORMALISED SPECTRA. $\theta_i = 140°$

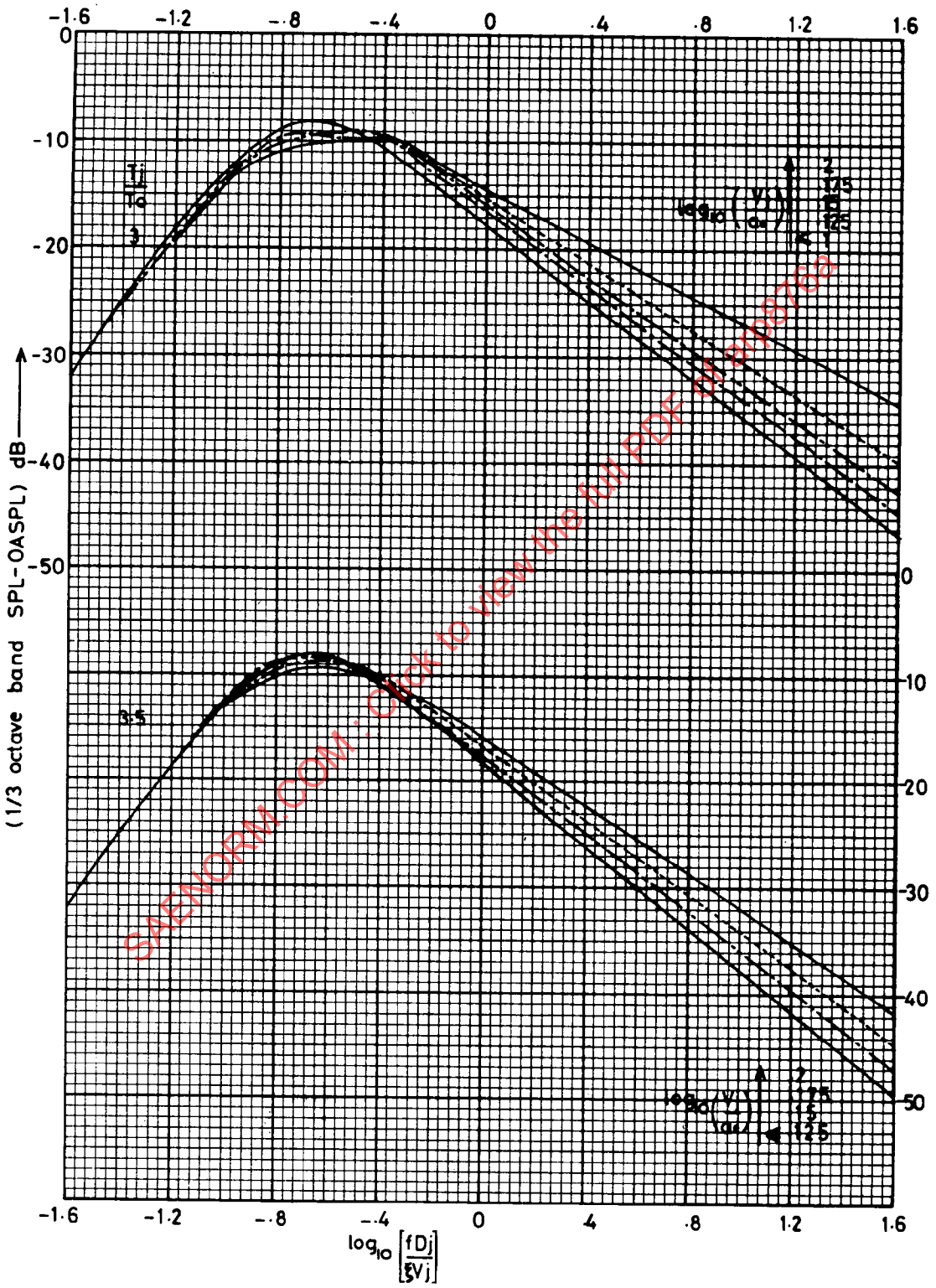

FIG. A10.

1/3 OCTAVE BAND NORMALISED SPECTRA. $\theta_i = 150°$

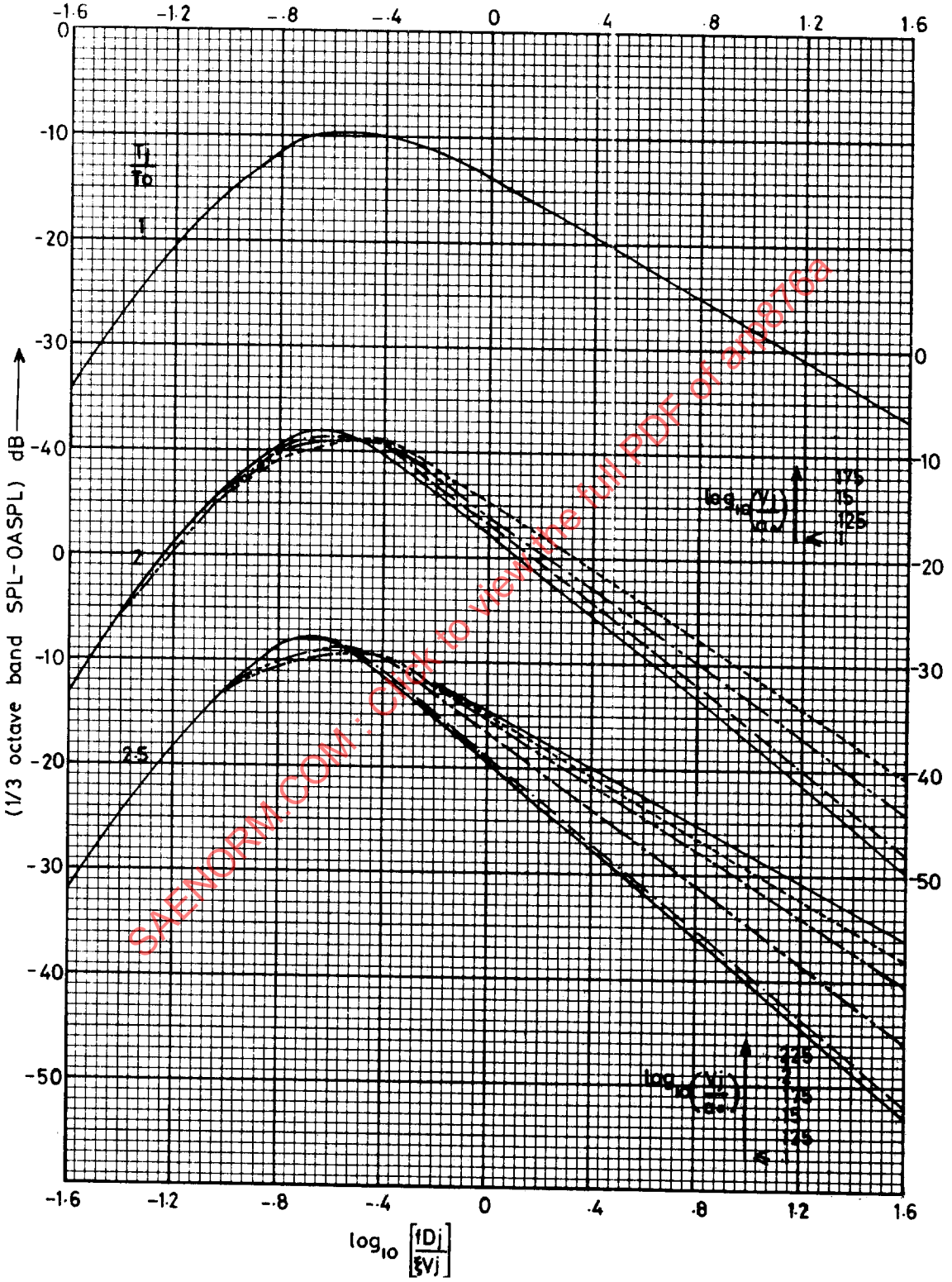

FIG. A10. (CONT'D)

1/3 OCTAVE BAND NORMALISED SPECTRA. $\theta_i = 150°$

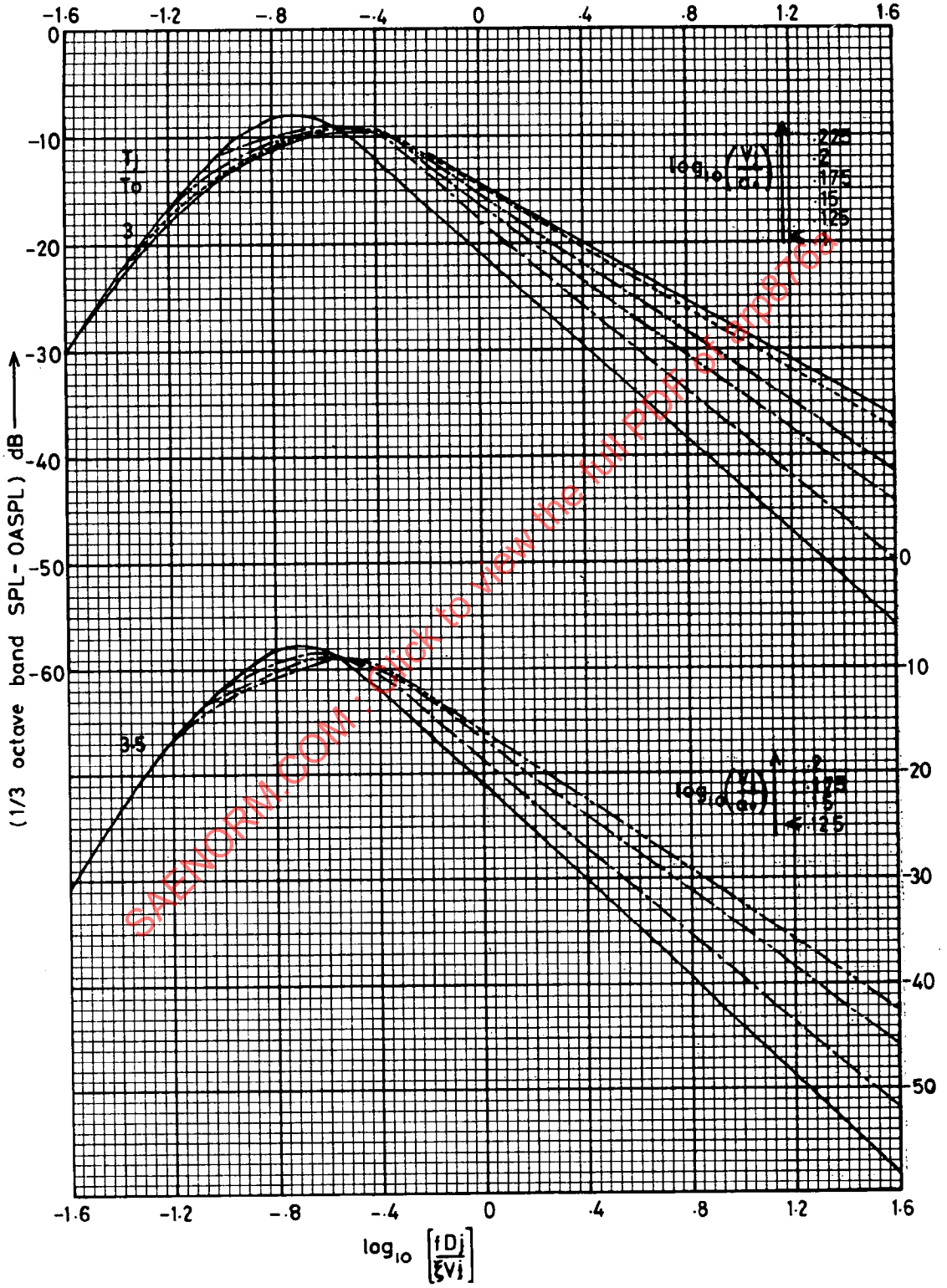

FIG. A11.

1/3 OCTAVE BAND NORMALISED SPECTRA. $\theta_i = 160°$

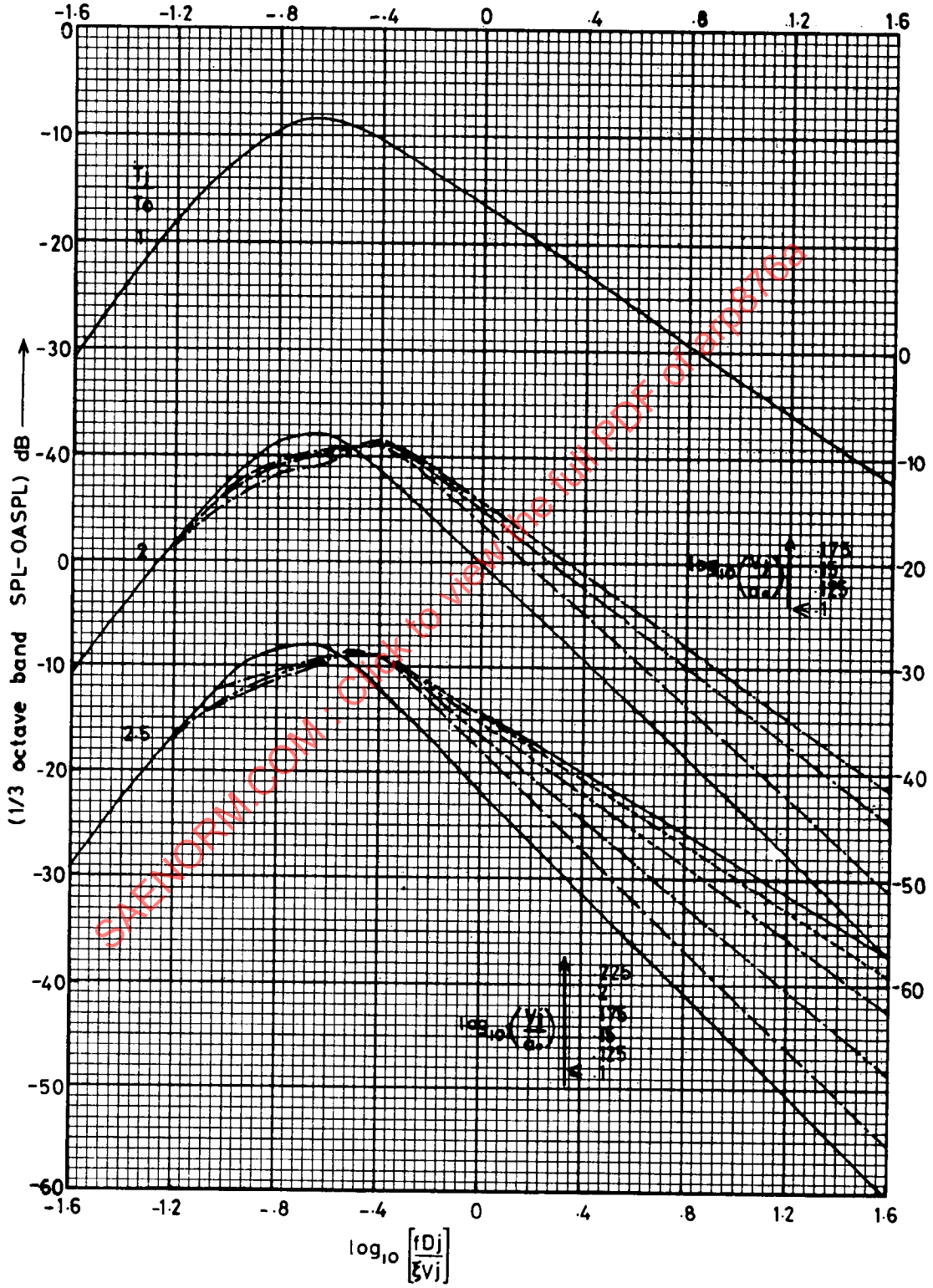

FIG. A11. (CONT'D)

1/3 OCTAVE BAND NORMALISED SPECTRA. $\theta_i = 160°$

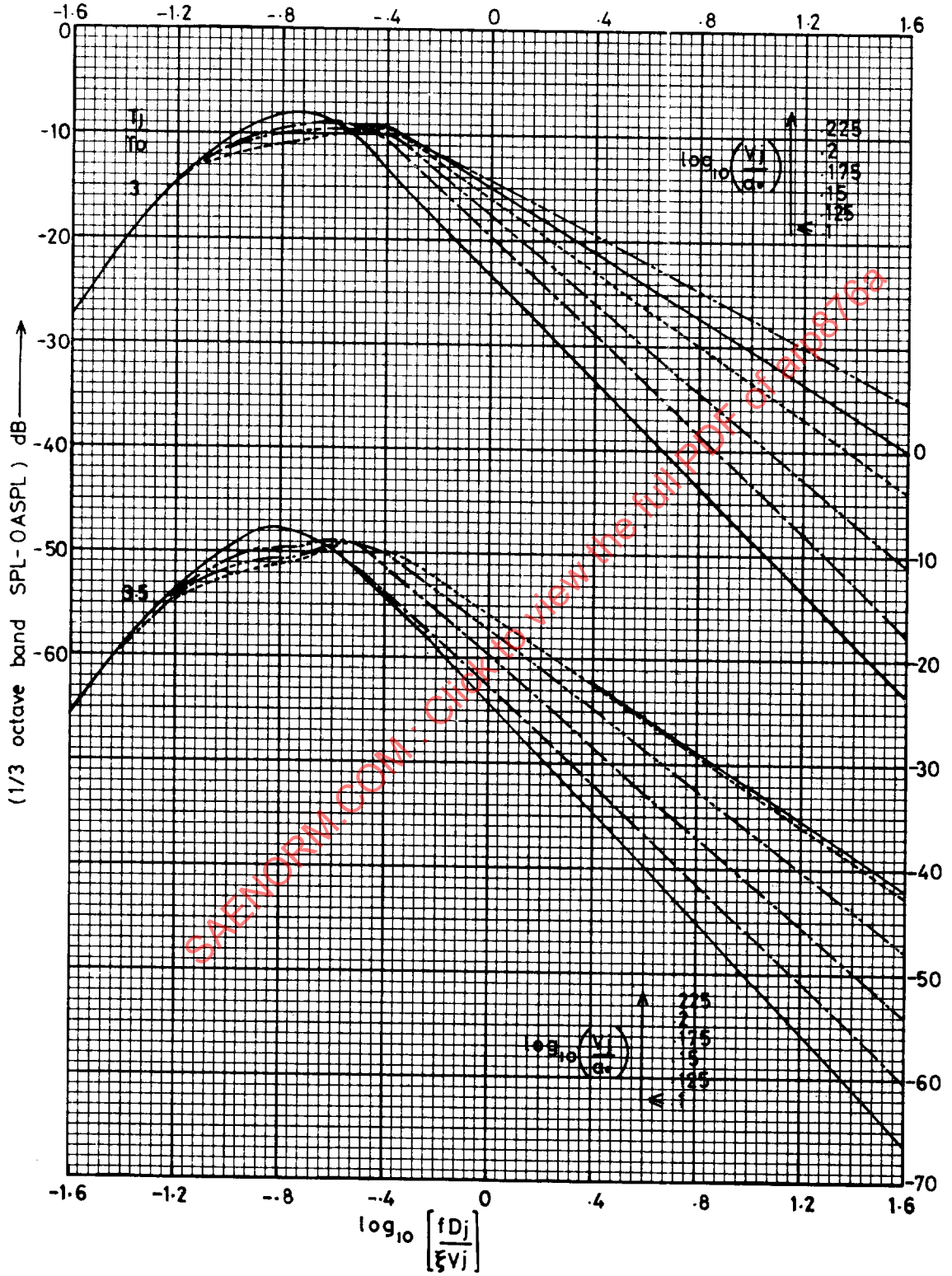

TABLE A1

VARIABLE DENSITY INDEX ω
(REF. FIG. A1)

$\text{Log}_{10}\left\{\frac{V_j}{a_o}\right\}$	ω
-.4	-.90
-.35	-.76
-.3	-.58
-.25	-.41
-.20	-.22
-.15	0
-.10	+.22
-.05	+.50
0	+.77
+.05	+1.07
+.10	+1.39
+.15	+1.74
+.20	+1.95
+.25	+2.0
+.30	+2.0
+.35	+2.0
+.40	+2.0

Note:- The values of ω in this table have been derived from rig data where jet temperature Tj varies from 288°K to 1100°K.

PURE JET MIXING NOISE
NON-DIMENSIONAL POLAR OASPL VALUES (REF. FIG. A2)

TABLE A2

$\log_{10}\left\{\frac{V_j}{a_o}\right\}$	Θ_i, Angle to Inlet														
	20	30	40	50	60	70	80	90	100	110	120	130	140	150	160
-.4	106.6	107.0	107.2	107.5	108.0	108.4	108.8	109.5	110.2	111.2	112.3	113.2	114.0	114.6	114.9
-.35	110.1	110.5	111.0	111.3	111.5	112.1	112.5	113.2	113.9	115.0	116.1	117.2	118.2	118.7	119.2
-.30	113.7	114.1	114.5	115.0	115.4	115.8	116.3	116.8	117.7	118.7	120.0	121.2	122.2	122.9	123.4
-.25	117.3	117.7	118.2	118.5	118.8	119.4	120.0	120.6	121.5	122.6	123.9	125.3	126.5	127.3	127.7
-.20	121.0	121.3	121.7	122.0	122.5	123.0	123.6	124.3	125.3	126.5	128.0	129.5	130.6	131.5	131.9
-.15	124.7	125.0	125.5	125.8	126.2	126.6	127.3	128.1	129.2	130.5	132.1	133.8	135.0	136.0	136.3
-.10	128.4	128.7	129.1	129.5	130.0	130.4	131.0	131.8	133.0	134.5	136.4	138.0	139.5	140.4	140.7
-.05	132.1	132.4	132.8	133.1	133.7	133.9	134.7	135.7	136.9	138.7	140.7	142.7	144.3	145.4	145.3
0	136.0	136.1	136.4	136.7	137.1	137.7	138.4	139.4	140.9	142.8	145.0	147.5	149.3	150.4	150.2
+.05	139.9	140.0	140.3	140.6	141.0	141.4	142.3	143.3	145.0	147.1	149.6	152.3	154.8	156.1	155.4
+.10	143.9	144.0	144.1	144.3	144.6	145.2	146.1	147.4	149.0	151.4	154.2	157.4	160.3	161.9	161.0
+.15	147.5	147.8	148.0	148.3	148.8	149.3	150.3	151.5	153.3	155.8	159.0	162.8	165.8	167.0	165.8
+.20	151.3	151.5	151.9	152.4	152.9	153.7	154.6	155.9	157.7	160.4	164.2	168.5	171.1	171.3	170.0
+.25	154.8	155.2	155.5	156.0	156.7	157.5	158.5	159.9	161.7	164.8	168.8	173.6	175.7	174.9	172.6
+.30	158.1	158.5	159.0	159.5	160.2	161.1	162.2	163.7	165.8	168.9	173.4	178.0	179.6	177.8	174.6
+.35	161.3	161.6	162.1	162.7	163.3	164.3	165.5	167.1	169.3	172.7	177.2	181.5	182.5	180.1	176.2
+.4	164.3	164.5	164.9	165.4	166.0	167.0	168.3	170.0	172.5	176.4	180.6	184.2	183.8	181.4	177.5

TABLE A3

$\frac{(V_i)}{(a_o)}$	Values of ξ (ref. Fig. A3)					
	$\theta_i \leq 120°$	130°	135°	140°	150°	160°
1.4	1.0	1.0	1.0	1.0	1.0	1.0
1.5	1.0	1.0	1.0	1.0	1.0	.995
1.6	1.0	1.0	1.0	1.0	1.0	.885
1.7	1.0	1.0	1.0	1.0	.965	.76
1.8	1.0	1.0	1.0	.99	.87	.66
1.9	1.0	1.0	1.0	.95	.775	.59
2.0	1.0	1.0	.981	.90	.71	.54
2.1	1.0	1.0	.955	.86	.66	.5
2.2	1.0	1.0	.920	.83	.63	.47
2.3	1.0	.985	.895	.81	.61	.445
2.4	1.0	.970	.88	.795	.595	.43
2.5	1.0	.955	.87	.79	.59	.420

For $\left\{\frac{V_i}{a_o}\right\} < 1.4$, $\xi = 1.0$

Table A4

GAS TURBINE JET EXHAUST NOISE PREDICTION

θ_i ANGLE TO INTAKE = 90.00 DEGREES

$\log_{10}\left[\frac{fDj}{\xi Vj}\right]$	1/3RD OCTAVE BAND SOUND PRESSURE LEVEL (SPL-OASPL) DB				
-1.60	-32.95	-30.09	-30.12	-30.33	-30.23
-1.50	-30.75	-27.91	-27.88	-28.15	-28.04
-1.40	-28.53	-25.83	-25.71	-25.96	-25.81
-1.30	-26.35	-23.79	-23.62	-23.83	-23.63
-1.20	-24.31	-21.77	-21.66	-21.85	-21.57
-1.10	-22.04	-19.85	-19.80	-19.73	-19.41
-1.00	-19.65	-18.09	-18.02	-17.53	-17.23
-0.90	-17.95	-16.64	-16.39	-15.73	-15.47
-0.80	-16.50	-15.24	-14.86	-14.19	-14.00
-0.70	-15.16	-13.80	-13.43	-12.94	-12.84
-0.60	-14.13	-12.57	-12.40	-11.91	-11.81
-0.50	-13.05	-11.79	-11.52	-11.23	-11.23
-0.40	-12.25	-11.30	-11.03	-10.93	-10.83
-0.30	-11.84	-10.99	-10.82	-10.93	-10.83
-0.20	-11.42	-11.00	-10.88	-11.07	-10.84
-0.10	-11.35	-11.12	-11.10	-11.24	-11.13
0.0	-11.35	-11.40	-11.42	-11.53	-11.63
0.10	-11.46	-11.84	-11.94	-12.04	-12.20
0.20	-11.73	-12.44	-12.60	-12.71	-12.86
0.30	-12.24	-13.16	-13.37	-13.51	-13.62
0.40	-12.79	-13.96	-14.23	-14.40	-14.49
0.50	-13.39	-14.79	-15.14	-15.36	-15.46
0.60	-14.08	-15.68	-16.13	-16.40	-16.62
0.70	-14.90	-16.63	-17.20	-17.55	-17.93
0.80	-15.81	-17.64	-18.33	-18.75	-19.33
0.90	-16.80	-18.70	-19.51	-19.99	-20.75
1.00	-17.85	-19.80	-20.72	-21.23	-22.13
1.10	-18.94	-20.95	-21.96	-22.48	-23.45
1.20	-20.10	-22.13	-23.24	-23.74	-24.78
1.30	-21.32	-23.36	-24.55	-25.03	-26.12
1.40	-22.60	-24.63	-25.91	-26.34	-27.45
1.50	-23.94	-25.95	-27.29	-27.68	-28.79
1.60	-25.35	-27.31	-28.72	-29.03	-30.13
(TJ/TO)	1.00	2.00	2.50	3.00	3.50
LOG(VJ/AO)	≤ 0.400	≤0.400	≤0.400	≤0.400	≤0.400

Table A5

GAS TURBINE JET EXHAUST NOISE PREDICTION

θ, ANGLE TO INTAKE = 100.00 DEGREES

$\log_{10}\left(\frac{fDj}{\xi Vj}\right)$	1/3RD OCTAVE BAND SOUND PRESSURE LEVEL (SPL-OASPL) DB				
-1.60	-33.07	-31.77	-31.12	-31.11	-30.96
-1.50	-30.81	-29.34	-28.67	-28.79	-28.66
-1.40	-28.56	-26.95	-26.34	-26.50	-26.33
-1.30	-26.37	-24.67	-24.12	-24.31	-24.06
-1.20	-24.32	-22.66	-22.09	-22.31	-21.95
-1.10	-22.13	-20.17	-20.13	-20.25	-19.65
-1.00	-19.87	-17.47	-18.22	-18.10	-17.26
-0.90	-18.06	-16.26	-16.47	-16.04	-15.44
-0.80	-16.53	-15.13	-14.83	-14.21	-13.91
-0.70	-15.28	-13.58	-13.33	-12.82	-12.67
-0.60	-14.15	-12.45	-12.20	-11.69	-11.85
-0.50	-13.37	-11.47	-11.42	-10.91	-11.26
-0.40	-12.39	-10.78	-10.82	-10.61	-10.87
-0.30	-11.67	-10.57	-10.72	-10.61	-10.66
-0.20	-11.27	-10.58	-10.73	-10.75	-10.81
-0.10	-11.27	-10.92	-10.97	-11.16	-11.11
0.0	-11.27	-11.47	-11.42	-11.71	-11.56
0.10	-11.40	-12.09	-11.99	-12.33	-12.15
0.20	-11.74	-12.82	-12.70	-13.04	-12.86
0.30	-12.23	-13.63	-13.52	-13.82	-13.67
0.40	-12.80	-14.49	-14.41	-14.68	-14.59
0.50	-13.42	-15.38	-15.33	-15.63	-15.61
0.60	-14.12	-16.32	-16.32	-16.68	-16.78
0.70	-14.93	-17.30	-17.37	-17.83	-18.07
0.80	-15.84	-18.33	-18.48	-19.03	-19.43
0.90	-16.83	-19.39	-19.63	-20.27	-20.81
1.00	-17.87	-20.48	-20.82	-21.51	-22.16
1.10	-18.97	-21.59	-22.04	-22.75	-23.48
1.20	-20.13	-22.73	-23.30	-24.02	-24.81
1.30	-21.35	-23.90	-24.60	-25.31	-26.14
1.40	-22.63	-25.10	-25.93	-26.62	-27.48
1.50	-23.97	-26.33	-27.31	-27.95	-28.82
1.60	-25.37	-27.58	-28.72	-29.31	-30.16
(TJ/TO)	1.00	2.00	2.50	3.00	3.50
LOG(VJ/AO)	≤0.400	≤0.400	≤0.400	≤0.400	≤0.400

Table A6

GAS TURBINE JET EXHAUST NOISE PREDICTION

θ_t ANGLE TO INTAKE = 110.00 DEGREES

$\log_{10}\left(\frac{fDj}{\xi Vj}\right)$	1/3RD OCTAVE BAND SOUND PRESSURE LEVEL (SPL-OASPL) DB				
-1.60	-34.57	-32.82	-32.12	-32.30	-32.03
-1.50	-32.12	-30.26	-29.55	-30.12	-29.36
-1.40	-29.69	-27.74	-27.08	-28.14	-26.64
-1.30	-27.27	-25.32	-24.72	-26.00	-24.03
-1.20	-24.87	-23.10	-22.58	-23.43	-21.69
-1.10	-22.40	-20.93	-20.41	-20.73	-19.26
-1.00	-19.97	-18.82	-18.22	-18.10	-16.83
-0.90	-18.18	-16.93	-16.26	-16.04	-15.17
-0.80	-16.57	-15.24	-14.54	-14.31	-13.82
-0.70	-14.98	-13.84	-13.14	-12.81	-12.64
-0.60	-13.75	-12.60	-12.10	-10.80	-11.52
-0.50	-12.67	-11.53	-11.22	-10.80	-11.03
-0.40	-12.08	-10.93	-10.63	-10.70	-10.64
-0.30	-11.57	-10.63	-10.52	-10.50	-10.53
-0.20	-11.45	-10.54	-10.67	-10.52	-10.69
-0.10	-11.39	-10.83	-10.92	-10.98	-11.02
0.0	-11.37	-11.33	-11.32	-11.70	-11.53
0.10	-11.50	-11.90	-11.96	-12.40	-12.24
0.20	-11.83	-12.56	-12.79	-13.16	-13.12
0.30	-12.32	-13.32	-13.73	-13.99	-14.11
0.40	-12.90	-14.15	-14.74	-14.91	-15.18
0.50	-13.51	-15.05	-15.76	-15.95	-16.29
0.60	-14.21	-16.04	-16.81	-17.14	-17.48
0.70	-15.03	-17.13	-17.93	-18.44	-18.76
0.80	-15.94	-18.26	-19.08	-19.81	-20.08
0.90	-16.93	-19.41	-20.25	-21.18	-21.42
1.00	-17.97	-20.54	-21.42	-22.50	-22.73
1.10	-19.06	-21.65	-22.59	-23.77	-24.02
1.20	-20.22	-22.78	-23.77	-25.03	-25.32
1.30	-21.44	-23.91	-24.97	-26.29	-26.62
1.40	-22.72	-25.04	-26.17	-27.53	-27.92
1.50	-24.06	-26.19	-27.39	-28.77	-29.22
1.60	-25.47	-27.34	-28.62	-30.00	-30.53

(TJ/TO)	1.00	2.00	2.50	3.00	3.50
LOG(VJ/AO)	≤0.400	≤0.400	≤0.400	≤0.400	≤0.400

Table A7

GAS TURBINE JET EXHAUST NOISE PREDICTION

θ_i ANGLE TO INTAKE = 120.00 DEGREES

$\log_{10}\left(\frac{fDj}{Vj}\right)$	1/3RD OCTAVE BAND SOUND PRESSURE LEVEL (SPL-OASPL) DB				
-1.60	-36.37	-33.75	-33.11	-32.50	-32.27
-1.50	-33.31	-31.00	-30.17	-29.66	-29.32
-1.40	-30.18	-28.25	-27.25	-26.97	-26.44
-1.30	-27.27	-25.65	-24.51	-24.50	-23.66
-1.20	-24.82	-23.35	-22.16	-22.52	-21.11
-1.10	-22.49	-21.13	-19.75	-20.30	-18.56
-1.00	-20.27	-18.95	-17.31	-17.80	-16.06
-0.90	-18.50	-16.88	-15.31	-15.63	-13.99
-0.80	-16.87	-15.05	-13.63	-13.82	-12.31
-0.70	-15.29	-13.66	-12.32	-12.51	-11.17
-0.60	-14.05	-12.43	-11.29	-11.28	-10.45
-0.50	-13.07	-11.35	-10.61	-10.60	-10.06
-0.40	-12.28	-10.76	-10.31	-10.30	-9.97
-0.30	-11.77	-10.46	-10.31	-10.30	-10.17
-0.20	-11.53	-10.37	-10.47	-10.46	-10.71
-0.10	-11.35	-10.65	-10.98	-10.88	-11.40
0.0	-11.27	-11.15	-11.71	-11.59	-12.27
0.10	-11.39	-11.79	-12.56	-12.29	-13.38
0.20	-11.71	-12.55	-13.54	-13.23	-14.67
0.30	-12.17	-13.42	-14.61	-14.30	-16.06
0.40	-12.72	-14.38	-15.74	-15.46	-17.49
0.50	-13.31	-15.41	-16.87	-16.69	-18.89
0.60	-14.01	-16.55	-18.03	-18.04	-20.29
0.70	-14.82	-17.79	-19.24	-19.50	-21.72
0.80	-15.74	-19.08	-20.48	-21.02	-23.17
0.90	-16.73	-20.39	-21.74	-22.56	-24.62
1.00	-17.77	-21.67	-23.00	-24.10	-26.07
1.10	-18.87	-22.94	-24.28	-25.63	-27.51
1.20	-20.02	-24.21	-25.58	-27.17	-28.96
1.30	-21.24	-25.49	-26.88	-28.73	-30.41
1.40	-22.52	-26.78	-28.21	-30.31	-31.86
1.50	-23.87	-28.08	-29.55	-31.90	-33.31
1.60	-25.27	-29.38	-30.90	-33.50	-34.77
(TJ/TO)	1.00	2.00	2.50	3.00	3.50
LOG(VJ/AO)	≤0.400	≤0.400	≤0.400	≤0.400	≤0.400

Table A8

GAS TURBINE JET EXHAUST NOISE PREDICTION

θ_i ANGLE TO INTAKE = 130.00 DEGREES

$\log_{10}\left[\frac{fDj}{\xi Vj}\right]$	1/3RD OCTAVE BAND SOUND PRESSURE LEVEL (SPL-OASPL) DB									
-1.60	-35.40	-34.33	-33.16	-32.65	-32.67	-32.69	-32.70	-33.44	-33.44	-33.45
-1.50	-32.25	-31.23	-29.91	-29.53	-29.55	-29.57	-29.58	-30.18	-30.18	-30.19
-1.40	-29.26	-28.17	-26.69	-26.54	-26.55	-26.57	-26.59	-26.93	-26.93	-26.94
-1.30	-26.50	-25.23	-23.66	-23.65	-23.67	-23.69	-23.70	-23.74	-23.74	-23.75
-1.20	-24.17	-22.51	-21.01	-21.04	-21.05	-21.08	-21.09	-20.69	-20.69	-20.70
-1.10	-22.02	-19.97	-18.51	-18.01	-18.02	-18.04	-18.06	-17.45	-17.45	-17.46
-1.00	-20.00	-17.63	-16.16	-14.65	-14.66	-14.69	-14.70	-14.14	-14.14	-14.15
-0.90	-18.24	-15.60	-14.14	-11.87	-11.88	-11.90	-12.58	-11.37	-11.37	-11.50
-0.80	-16.60	-13.82	-12.35	-10.05	-10.06	-10.08	-11.15	-9.51	-9.51	-9.70
-0.70	-15.01	-12.34	-10.87	-9.36	-9.37	-9.39	-9.71	-8.74	-8.74	-8.75
-0.60	-13.77	-11.21	-10.15	-9.15	-9.16	-9.19	-8.70	-8.64	-8.64	-8.65
-0.50	-12.50	-10.43	-9.76	-9.25	-9.27	-9.29	-9.00	-9.04	-9.04	-8.95
-0.40	-11.61	-10.14	-9.86	-9.94	-9.95	-9.97	-9.78	-10.21	-10.21	-10.23
-0.30	-10.99	-10.14	-10.17	-10.87	-10.88	-10.90	-10.91	-11.45	-11.45	-11.46
-0.20	-10.80	-10.21	-10.84	-11.92	-11.93	-11.95	-11.97	-12.64	-12.64	-12.65
-0.10	-10.84	-10.70	-11.73	-13.25	-13.26	-13.28	-13.29	-14.15	-14.15	-14.16
0.0	-11.00	-11.44	-12.76	-14.66	-14.67	-14.69	-14.70	-15.74	-15.74	-15.75
0.10	-11.35	-12.40	-13.89	-16.08	-16.08	-16.08	-16.02	-17.30	-17.31	-17.25
0.20	-11.91	-13.54	-15.06	-17.54	-17.50	-17.45	-17.20	-18.87	-18.88	-18.68
0.30	-12.61	-14.80	-16.27	-19.01	-18.92	-18.80	-18.31	-20.44	-20.45	-20.06
0.40	-13.33	-16.13	-17.50	-20.50	-20.36	-20.15	-19.41	-22.02	-22.03	-21.45
0.50	-14.18	-17.46	-18.75	-22.00	-21.80	-21.50	-20.58	-23.61	-23.60	-22.89
0.60	-15.02	-18.83	-20.04	-23.51	-23.25	-22.85	-21.79	-25.19	-25.17	-24.37
0.70	-15.93	-20.27	-21.36	-25.03	-24.73	-24.19	-23.01	-26.77	-26.73	-25.86
0.80	-16.89	-21.73	-22.69	-26.56	-26.21	-25.53	-24.24	-28.35	-28.30	-27.36
0.90	-17.92	-23.21	-24.03	-28.11	-27.69	-26.86	-25.47	-29.94	-29.87	-28.86
1.00	-19.00	-24.66	-25.36	-29.66	-29.17	-28.19	-26.71	-31.54	-31.44	-30.35
1.10	-20.12	-26.09	-26.67	-31.22	-30.66	-29.53	-27.95	-33.15	-33.02	-31.83
1.20	-21.30	-27.53	-27.97	-32.79	-32.16	-30.87	-29.18	-34.76	-34.60	-33.31
1.30	-22.52	-28.96	-29.27	-34.37	-33.66	-32.20	-30.44	-36.38	-36.19	-34.78
1.40	-23.80	-30.39	-30.57	-35.96	-35.16	-33.53	-31.69	-37.99	-37.77	-36.24
1.50	-25.12	-31.83	-31.86	-37.55	-36.67	-34.87	-32.95	-39.61	-39.36	-37.70
1.60	-26.50	-33.25	-33.15	-39.16	-38.18	-36.20	-34.21	-41.24	-40.95	-39.16
(TJ/TO)	1.00	2.00	2.50	3.00	3.00	3.00	3.00	3.50	3.50	3.50
LOG(VJ/AO)	≤0.400	≤0.400	≤0.400	≤0.125	0.150	0.175	0.200	≤0.150	0.175	0.200

Table A9

GAS TURBINE JET EXHAUST NOISE PREDICTION

θ_i ANGLE TO INTAKE = 140.00 DEGREES

$\log_{10}\left(\frac{fDj}{\sqrt{Vj}}\right)$	1/3RD OCTAVE BAND SOUND PRESSURE LEVEL (SPL-OASPL) DB										
-1.60	-35.00	-32.65	-32.39	-32.45	-32.63	-32.73	-32.80	-31.96	-31.60	-31.66	-31.67	-31.77
-1.50	-31.51	-29.09	-28.90	-28.95	-29.14	-29.23	-29.30	-28.59	-28.23	-28.29	-28.30	-28.40
-1.40	-28.16	-25.66	-25.43	-25.49	-25.67	-25.77	-25.84	-25.30	-24.94	-25.00	-25.01	-25.10
-1.30	-25.10	-22.55	-22.19	-22.25	-22.43	-22.53	-22.60	-22.16	-21.80	-21.86	-21.87	-21.97
-1.20	-22.65	-20.10	-19.42	-19.48	-19.66	-19.76	-19.83	-19.41	-19.06	-19.12	-19.13	-19.22
-1.10	-20.28	-17.68	-16.69	-16.75	-16.93	-17.03	-17.09	-16.17	-15.84	-15.96	-16.01	-16.16
-1.00	-17.90	-15.24	-13.99	-14.05	-14.23	-14.33	-14.40	-12.66	-12.50	-12.96	-13.07	-13.47
-0.90	-15.85	-13.31	-11.73	-12.14	-12.33	-12.43	-12.49	-10.35	-10.70	-11.18	-11.45	-12.01
-0.80	-14.15	-11.64	-10.08	-10.73	-10.92	-11.01	-11.08	-9.88	-9.70	-10.13	-10.47	-11.04
-0.70	-12.92	-10.25	-9.20	-9.85	-10.04	-10.14	-10.20	-8.26	-9.30	-9.56	-9.97	-10.46
-0.60	-11.53	-9.64	-8.99	-9.24	-9.43	-9.53	-9.59	-8.26	-9.70	-9.25	-9.56	-10.06
-0.50	-10.60	-9.45	-9.09	-9.15	-9.33	-9.43	-9.50	-9.16	-8.30	-8.76	-9.17	-9.57
-0.40	-10.21	-9.74	-9.88	-9.54	-9.62	-9.72	-9.79	-10.63	-9.77	-9.33	-9.36	-9.46
-0.30	-9.90	-10.16	-10.90	-10.26	-10.24	-10.34	-10.41	-12.48	-11.33	-11.08	-10.49	-10.38
-0.20	-10.19	-10.97	-12.20	-11.76	-11.42	-11.49	-11.35	-14.14	-13.17	-12.74	-12.25	-11.76
-0.10	-10.64	-12.02	-13.65	-13.21	-12.78	-12.67	-12.63	-15.88	-14.70	-14.35	-13.89	-13.02
0.0	-11.30	-13.26	-15.19	-14.75	-14.23	-13.93	-14.00	-17.66	-16.31	-15.97	-15.28	-14.27
0.10	-12.23	-14.63	-16.82	-16.33	-15.76	-15.33	-15.33	-19.47	-18.15	-17.65	-16.78	-15.56
0.20	-13.37	-16.22	-18.52	-17.89	-17.35	-16.81	-16.67	-21.30	-20.06	-19.35	-18.27	-16.87
0.30	-14.63	-17.84	-20.24	-19.46	-18.96	-18.33	-18.00	-23.13	-21.99	-21.06	-19.75	-18.18
0.40	-15.93	-19.49	-21.97	-21.07	-20.59	-19.86	-19.35	-24.97	-23.90	-22.77	-21.23	-19.48
0.50	-17.19	-21.15	-23.68	-22.75	-22.21	-21.38	-20.71	-25.77	-25.72	-24.46	-22.73	-20.76
0.60	-18.45	-22.83	-25.38	-24.45	-23.82	-22.89	-22.09	-28.56	-27.44	-26.14	-24.23	-22.02
0.70	-19.76	-24.55	-27.08	-26.14	-25.45	-24.42	-23.47	-30.33	-29.07	-27.81	-25.74	-23.26
0.80	-21.08	-26.28	-28.78	-27.85	-27.07	-25.95	-24.87	-32.10	-30.67	-29.47	-27.26	-24.49
0.90	-22.40	-28.03	-30.48	-29.55	-28.71	-27.49	-26.28	-33.87	-32.27	-31.13	-28.77	-25.73
1.00	-23.70	-29.77	-32.19	-31.26	-30.34	-29.03	-27.70	-33.66	-33.92	-32.78	-30.29	-26.97
1.10	-24.99	-31.51	-33.90	-32.96	-31.97	-30.58	-29.14	-37.47	-35.61	-34.42	-31.80	-28.22
1.20	-26.28	-33.25	-35.61	-34.66	-33.60	-32.14	-30.59	-39.29	-37.33	-36.05	-33.32	-29.47
1.30	-27.57	-35.00	-37.33	-36.36	-35.23	-33.70	-32.05	-41.12	-39.06	-37.67	-34.83	-30.72
1.40	-28.85	-36.76	-39.05	-38.06	-36.87	-35.27	-33.52	-42.96	-40.79	-39.28	-36.35	-31.97
1.50	-30.13	-38.51	-40.77	-39.76	-38.50	-36.85	-35.00	-44.81	-42.55	-40.89	-37.87	-33.22
1.60	-31.40	-40.28	-42.49	-41.46	-40.14	-38.43	-36.50	-46.66	-44.32	-42.48	-39.39	-34.47
(TJ/TC)	1.00	2.00	2.50	2.50	2.50	2.50	2.50	3.00	3.00	3.00	3.00	3.00
LOG(VJ/AO)	≤0.400	≤0.400	≤0.125	0.150	0.175	0.200	0.225	≤0.100	0.125	0.150	0.175	0.200

Table A9 (continued)

GAS TURBINE JET EXHAUST NOISE PREDICTION

θ_i ANGLE TO INTAKE = 140.00 DEGREES

$\log_{10}\left[\frac{fDj}{\xi Vj}\right]$	1/3RD OCTAVE BAND SOUND PRESSURE LEVEL (SPL-OASPL) DB				
-1.60	-32.16	-32.14	-31.97	-31.89	-31.75
-1.50	-28.71	-28.69	-28.52	-28.44	-28.30
-1.40	-25.31	-25.29	-25.12	-25.04	-24.90
-1.30	-22.06	-22.04	-21.87	-21.79	-21.65
-1.20	-19.13	-19.11	-18.94	-18.86	-18.72
-1.10	-16.03	-16.02	-15.85	-15.77	-15.63
-1.00	-12.86	-12.84	-12.77	-12.69	-12.65
-0.90	-10.32	-10.34	-10.68	-10.75	-11.08
-0.80	-8.67	-8.77	-9.28	-9.69	-10.27
-0.70	-8.05	-8.24	-8.57	-9.29	-9.85
-0.60	-8.16	-8.24	-8.37	-8.58	-9.13
-0.50	-8.76	-8.64	-8.57	-8.59	-8.45
-0.40	-10.82	-10.70	-10.03	-9.96	-9.82
-0.30	-12.88	-12.66	-12.39	-11.61	-11.17
-0.20	-14.67	-14.55	-14.18	-13.39	-12.81
-0.10	-16.61	-16.43	-15.99	-15.16	-14.39
0.0	-18.56	-18.35	-17.78	-16.89	-15.95
0.10	-20.47	-20.27	-19.56	-18.64	-17.54
0.20	-22.37	-22.19	-21.33	-20.39	-19.12
0.30	-24.27	-24.12	-23.10	-22.13	-20.72
0.40	-26.18	-26.05	-24.88	-23.85	-22.32
0.50	-28.11	-27.99	-26.70	-25.59	-23.92
0.60	-30.07	-29.94	-28.56	-27.30	-25.54
0.70	-32.04	-31.90	-30.44	-28.99	-27.17
0.80	-34.03	-33.86	-32.34	-30.67	-28.81
0.90	-36.00	-35.81	-34.22	-32.37	-30.44
1.00	-37.96	-37.75	-36.09	-34.10	-32.06
1.10	-39.90	-39.67	-37.93	-35.84	-33.67
1.20	-41.83	-41.58	-39.76	-37.60	-35.27
1.30	-43.75	-43.49	-41.58	-39.36	-36.88
1.40	-45.66	-45.39	-43.40	-41.13	-38.48
1.50	-47.57	-47.27	-45.20	-42.91	-40.07
1.60	-49.46	-49.15	-46.99	-44.70	-41.66
(TJ/TO)	3.50	3.50	3.50	3.50	3.50
LOG(VJ/A0)	≤ 0.100	0.125	0.150	0.175	0.200

Table A10

GAS TURBINE JET EXHAUST NOISE PREDICTION

θ_i ANGLE TO INTAKE = 150.00 DEGREES

$\log_{10}\left(\frac{fDj}{\xi Vj}\right)$	1/3RD OCTAVE BAND SOUND PRESSURE LEVEL (SPL-OASPL) DB											
-1.60	-34.07	-33.04	-32.98	-33.20	-33.20	-31.93	-31.84	-31.40	-31.60	-31.74	-31.88	-29.85
-1.50	-30.40	-29.37	-29.30	-29.53	-29.52	-28.33	-28.24	-27.80	-28.00	-28.14	-28.27	-26.37
-1.40	-26.80	-25.71	-25.65	-25.88	-25.87	-24.72	-24.63	-24.19	-24.39	-24.53	-24.67	-23.07
-1.30	-23.47	-22.24	-22.18	-22.40	-22.40	-21.33	-21.24	-20.80	-21.00	-21.14	-21.28	-19.85
-1.20	-20.69	-19.09	-19.03	-19.26	-19.25	-18.42	-18.33	-17.89	-18.09	-18.23	-18.37	-16.65
-1.10	-17.95	-16.26	-16.20	-16.42	-16.45	-15.59	-15.50	-15.11	-15.31	-15.45	-15.58	-13.69
-1.00	-15.27	-13.74	-13.67	-13.90	-14.10	-12.83	-12.74	-12.70	-12.90	-13.04	-13.18	-11.15
-0.90	-13.13	-11.51	-11.55	-11.78	-12.20	-10.39	-10.33	-11.24	-11.56	-11.70	-11.84	-9.27
-0.80	-11.37	-9.62	-9.97	-10.20	-10.86	-8.57	-8.52	-10.26	-10.67	-10.81	-10.95	-8.17
-0.70	-10.07	-8.25	-9.18	-9.42	-10.22	-7.63	-7.94	-9.60	-10.00	-10.14	-10.28	-7.85
-0.60	-9.47	-7.75	-8.68	-8.91	-9.70	-7.74	-7.94	-8.68	-9.13	-9.33	-9.46	-8.37
-0.50	-9.47	-8.45	-8.48	-8.71	-9.41	-9.13	-9.14	-8.50	-8.90	-9.04	-9.18	-9.86
-0.40	-9.76	-10.22	-9.16	-8.98	-8.69	-11.29	-10.90	-9.37	-9.38	-9.52	-9.66	-12.10
-0.30	-10.27	-11.97	-10.91	-10.94	-10.13	-13.25	-12.86	-11.43	-11.02	-10.86	-10.83	-14.17
-0.20	-11.29	-13.88	-13.12	-12.50	-11.55	-15.23	-14.99	-13.20	-12.43	-12.26	-12.15	-16.54
-0.10	-12.32	-15.81	-14.96	-14.25	-13.17	-17.35	-17.02	-15.01	-14.02	-13.70	-13.47	-18.71
0.0	-13.47	-17.76	-16.81	-16.03	-14.81	-19.43	-19.05	-16.81	-15.60	-15.14	-14.78	-20.85
0.10	-14.82	-19.75	-18.71	-17.79	-16.41	-21.50	-21.09	-18.58	-17.11	-16.57	-16.08	-23.02
0.20	-16.29	-21.75	-20.63	-19.56	-18.00	-23.58	-23.15	-20.34	-18.59	-18.00	-17.38	-25.20
0.30	-17.81	-23.75	-22.57	-21.33	-19.59	-25.65	-25.21	-22.09	-20.06	-19.42	-18.67	-27.38
0.40	-19.33	-25.75	-24.51	-23.09	-21.18	-27.73	-27.27	-23.85	-21.54	-20.84	-19.97	-29.57
0.50	-20.79	-27.72	-26.46	-24.84	-22.78	-29.81	-29.32	-25.64	-23.06	-22.27	-21.28	-31.75
0.60	-22.20	-29.64	-28.41	-26.57	-24.40	-31.89	-31.38	-27.44	-24.61	-23.71	-22.60	-33.93
0.70	-23.59	-31.54	-30.36	-28.29	-26.04	-33.98	-33.40	-29.26	-26.18	-25.14	-23.91	-36.11
0.80	-24.97	-33.43	-32.31	-30.00	-27.67	-36.07	-35.44	-31.09	-27.77	-26.58	-25.24	-38.28
0.90	-26.36	-35.34	-34.26	-31.72	-29.30	-38.15	-37.49	-32.91	-29.35	-28.01	-26.56	-40.46
1.00	-27.77	-37.28	-36.23	-33.45	-30.91	-40.23	-39.55	-34.73	-30.91	-29.44	-27.88	-42.65
1.10	-29.19	-39.25	-38.18	-35.19	-32.51	-42.30	-41.62	-36.54	-32.46	-30.87	-29.20	-44.84
1.20	-30.63	-41.25	-40.13	-36.93	-34.11	-44.37	-43.69	-38.35	-34.00	-32.29	-30.51	-47.04
1.30	-32.07	-43.26	-42.06	-38.68	-35.69	-46.44	-45.75	-40.15	-35.54	-33.71	-31.83	-49.23
1.40	-33.53	-45.28	-43.99	-40.44	-37.27	-48.51	-47.81	-41.95	-37.07	-35.12	-33.15	-51.44
1.50	-34.99	-47.33	-45.91	-42.20	-38.85	-50.57	-49.88	-43.75	-38.59	-36.53	-34.45	-53.64
1.60	-36.47	-49.39	-47.84	-43.96	-40.41	-52.63	-51.95	-45.54	-40.11	-37.94	-35.78	-55.85
(TJ/TC)	1.00	2.00	2.00	2.00	2.00	2.50	2.50	2.50	2.50	2.50	2.50	3.00
LOG(VJ/A0)	≤0.400	≤0.100	0.125	0.150	0.175	≤0.100	0.125	0.150	0.175	0.200	0.225	≤0.100

Table A10 (continued)

GAS TURBINE JET EXHAUST NOISE PREDICTION

θ_i ANGLE TO INTAKE = 150.00 DEGREES

$\log_{10}\left(\frac{fDj}{\xi Vj}\right)$	1/3RD OCTAVE BAND SOUND PRESSURE LEVEL (SPL-OASPL) DB									
-1.60	-29.97	-29.98	-30.03	-30.02	-30.07	-30.64	-30.39	-30.40	-30.39	-30.40
-1.50	-26.49	-26.50	-26.56	-26.58	-26.65	-26.86	-26.81	-26.82	-26.82	-26.82
-1.40	-23.20	-23.21	-23.26	-23.38	-23.53	-23.14	-22.89	-22.90	-22.89	-22.92
-1.30	-19.97	-19.98	-20.03	-20.32	-20.56	-19.64	-19.39	-19.39	-19.39	-19.50
-1.20	-16.89	-17.06	-17.23	-17.53	-17.87	-16.61	-16.46	-16.74	-16.69	-16.82
-1.10	-14.06	-14.54	-14.90	-15.25	-15.51	-13.91	-13.97	-14.40	-14.57	-14.65
-1.00	-11.65	-12.47	-13.03	-13.52	-13.56	-11.53	-11.88	-12.29	-12.89	-12.90
-0.90	-10.69	-11.24	-11.74	-12.24	-12.27	-9.41	-10.31	-10.98	-11.63	-11.63
-0.80	-10.07	-10.38	-10.84	-11.33	-11.37	-8.15	-9.28	-10.09	-10.69	-10.70
-0.70	-9.27	-9.58	-10.14	-10.53	-10.57	-7.83	-8.58	-9.40	-9.90	-9.91
-0.60	-8.86	-9.07	-9.32	-9.51	-9.75	-8.25	-8.48	-8.78	-8.88	-8.88
-0.50	-8.87	-8.93	-9.13	-9.22	-9.37	-9.64	-8.79	-8.79	-8.79	-8.80
-0.40	-9.63	-9.45	-9.52	-9.51	-9.55	-11.90	-10.55	-9.97	-9.67	-9.67
-0.30	-11.70	-11.10	-10.55	-10.43	-10.38	-14.07	-12.72	-11.62	-11.11	-11.12
-0.20	-13.63	-12.88	-12.09	-11.83	-11.66	-16.57	-14.65	-13.30	-12.75	-12.75
-0.10	-15.65	-14.69	-13.77	-13.22	-13.00	-18.82	-16.72	-15.15	-14.37	-14.32
0.0	-17.68	-16.49	-15.44	-14.62	-14.37	-21.05	-18.80	-17.00	-16.00	-15.90
0.10	-19.74	-18.28	-17.05	-16.05	-15.76	-23.36	-20.86	-18.77	-17.62	-17.52
0.20	-21.81	-20.08	-18.64	-17.50	-17.17	-25.69	-22.92	-20.51	-19.25	-19.15
0.30	-23.87	-21.86	-20.22	-18.96	-18.59	-28.04	-24.98	-22.23	-20.88	-20.79
0.40	-25.93	-23.64	-21.81	-20.41	-20.00	-30.37	-27.03	-23.95	-22.52	-22.43
0.50	-27.96	-25.40	-23.41	-21.85	-21.38	-32.63	-29.09	-25.71	-24.18	-24.08
0.60	-29.95	-27.13	-25.03	-23.29	-22.73	-34.99	-31.14	-27.50	-25.86	-25.74
0.70	-31.92	-28.85	-26.65	-24.73	-24.07	-37.17	-33.19	-29.29	-27.55	-27.41
0.80	-33.87	-30.56	-28.28	-26.16	-25.39	-39.40	-35.23	-31.10	-29.24	-29.08
0.90	-35.83	-32.28	-29.91	-27.60	-26.72	-41.65	-37.28	-32.91	-30.93	-30.75
1.00	-37.80	-34.00	-31.54	-29.02	-28.07	-43.96	-39.32	-34.71	-32.60	-32.41
1.10	-39.79	-35.74	-33.18	-30.45	-29.43	-46.30	-41.36	-36.51	-34.25	-34.05
1.20	-41.79	-37.49	-34.81	-31.87	-30.81	-48.63	-43.40	-38.31	-35.90	-35.69
1.30	-43.79	-39.24	-36.44	-33.29	-32.19	-50.97	-45.44	-40.11	-37.54	-37.33
1.40	-45.79	-40.99	-38.08	-34.70	-33.57	-53.32	-47.47	-41.91	-39.17	-38.96
1.50	-47.80	-42.75	-39.71	-36.11	-34.97	-55.68	-49.51	-43.71	-40.79	-40.59
1.60	-49.81	-44.51	-41.35	-37.52	-36.37	-58.07	-51.54	-45.51	-42.40	-42.21
(TJ/TO)	3.00	3.00	3.00	3.00	3.00	3.50	3.50	3.50	3.50	3.50
LOG(VJ/AO)	0.125	0.150	0.175	0.200	0.225	≤0.125	0.150	0.175	0.200	0.225

Table A11

GAS TURBINE JET EXHAUST NOISE PREDICTION

θ_i ANGLE TO INTAKE = 160.00 DEGREES

$\log_{10}\left(\frac{fDj}{\bar{V}j}\right)$	1/3RD OCTAVE BAND SOUND PRESSURE LEVEL (SPL-OASPL) DB										
-1.60	-30.74	-30.49	-30.08	-30.50	-30.50	-29.05	-28.90	-29.05	-29.20	-29.38	-29.48	-27.13
-1.50	-27.37	-27.40	-26.99	-27.41	-27.41	-25.75	-25.60	-25.75	-25.90	-26.09	-26.18	-23.66
-1.40	-24.18	-24.31	-23.90	-24.33	-24.33	-22.51	-22.35	-22.50	-22.65	-22.84	-22.93	-20.28
-1.30	-21.14	-21.29	-20.88	-21.31	-21.31	-19.45	-19.30	-19.45	-19.60	-19.78	-19.88	-17.13
-1.20	-18.37	-18.44	-18.23	-18.66	-18.77	-16.84	-17.00	-17.09	-17.30	-17.49	-17.58	-14.35
-1.10	-15.68	-15.39	-15.70	-16.13	-16.41	-14.11	-14.54	-14.99	-15.24	-15.42	-15.52	-12.00
-1.00	-13.14	-12.29	-13.38	-13.81	-14.30	-11.35	-11.99	-13.15	-13.39	-13.58	-13.68	-10.13
-0.90	-11.17	-10.00	-11.55	-11.98	-12.81	-9.37	-11.30	-11.90	-12.34	-12.53	-12.62	-8.82
-0.80	-9.58	-8.52	-10.37	-10.80	-11.80	-8.13	-10.77	-10.92	-11.46	-11.65	-11.74	-8.15
-0.70	-8.54	-7.89	-9.88	-10.31	-11.31	-7.65	-10.00	-10.15	-10.60	-10.79	-10.88	-8.03
-0.60	-8.54	-7.89	-9.37	-9.79	-10.58	-8.07	-9.08	-9.23	-9.67	-9.86	-9.95	-8.66
-0.50	-9.24	-8.59	-8.88	-9.31	-9.31	-9.65	-8.40	-8.55	-8.69	-8.88	-8.97	-10.63
-0.40	-10.42	-11.34	-8.87	-8.80	-8.40	-12.30	-8.87	-8.82	-8.88	-9.07	-9.16	-13.38
-0.30	-11.76	-13.72	-9.92	-9.83	-9.32	-14.67	-10.73	-10.47	-10.21	-10.19	-10.29	-16.06
-0.20	-13.23	-15.83	-12.18	-11.40	-10.78	-16.86	-13.01	-12.38	-11.87	-11.61	-11.68	-18.37
-0.10	-14.85	-18.07	-14.30	-13.25	-12.53	-19.23	-15.35	-14.36	-13.58	-13.20	-13.09	-20.89
0.0	-16.44	-20.30	-16.41	-15.13	-14.31	-21.75	-17.71	-16.36	-15.30	-14.78	-14.47	-23.43
0.10	-18.04	-22.59	-18.56	-16.95	-16.01	-24.13	-20.08	-18.35	-16.98	-16.29	-15.86	-25.90
0.20	-19.66	-24.90	-20.73	-18.77	-17.68	-26.62	-22.45	-20.34	-18.66	-17.78	-17.23	-28.35
0.30	-21.27	-27.23	-22.90	-20.58	-19.34	-29.05	-24.83	-22.34	-20.33	-19.25	-18.60	-30.79
0.40	-22.89	-29.55	-25.07	-22.42	-21.01	-31.49	-27.20	-24.33	-22.01	-20.73	-19.99	-33.23
0.50	-24.52	-31.84	-27.23	-24.28	-22.70	-33.90	-29.56	-26.32	-23.69	-22.23	-21.40	-35.70
0.60	-26.14	-34.03	-29.37	-26.18	-24.42	-36.30	-31.90	-28.31	-25.37	-23.75	-22.84	-38.20
0.70	-27.77	-36.31	-31.51	-28.11	-26.14	-38.68	-34.24	-30.30	-27.05	-25.28	-24.30	-40.70
0.80	-29.41	-38.53	-33.65	-30.05	-27.87	-41.06	-36.56	-32.29	-28.73	-26.82	-25.77	-43.21
0.90	-31.03	-40.76	-35.80	-31.97	-29.59	-43.45	-38.89	-34.28	-30.41	-28.35	-27.23	-45.73
1.00	-32.64	-43.02	-37.95	-33.85	-31.31	-45.85	-41.23	-36.28	-32.10	-29.88	-28.68	-48.23
1.10	-34.24	-45.31	-40.11	-35.69	-33.02	-48.25	-43.56	-38.27	-33.80	-31.40	-30.10	-50.74
1.20	-35.84	-47.61	-42.28	-37.50	-34.73	-50.69	-45.90	-40.27	-35.49	-32.92	-31.51	-53.24
1.30	-37.42	-49.92	-44.44	-39.28	-36.43	-53.12	-48.23	-42.27	-37.19	-34.44	-32.92	-55.74
1.40	-39.00	-52.24	-46.61	-41.04	-38.13	-55.55	-50.57	-44.28	-38.89	-35.96	-34.31	-58.24
1.50	-40.58	-54.58	-48.79	-42.77	-39.82	-58.00	-52.90	-46.28	-40.60	-37.47	-35.70	-60.74
1.60	-42.14	-56.93	-50.97	-44.48	-41.51	-60.45	-55.24	-48.29	-42.31	-38.98	-37.08	-63.24
(TJ/TO)	1.00	2.00	2.00	2.00	2.00	2.50	2.50	2.50	2.50	2.50	2.50	3.00
LOG(VJ/AO)	≤0.400	≤0.100	0.125	0.150	0.175	≤0.100	0.125	0.150	0.175	0.200	0.225	≤0.100

Table A11 (continued)

GAS TURBINE JET EXHAUST NOISE PREDICTION

θ_i ANGLE TO INTAKE = 160.00 DEGREES

$\log_{10}\left(\frac{fDj}{\sqrt{Vj}}\right)$	1/3RD OCTAVE BAND SOUND PRESSURE LEVEL (SPL-OASPL) DB										
-1.60	-27.01	-26.93	-26.88	-26.90	-27.07	-25.49	-25.41	-25.88	-25.97	-25.76	-25.77
-1.50	-23.54	-23.46	-23.41	-23.43	-23.60	-22.09	-22.01	-22.48	-22.57	-22.36	-22.37
-1.40	-20.17	-20.08	-20.03	-20.06	-20.23	-18.82	-18.74	-19.21	-19.30	-19.09	-19.11
-1.30	-17.01	-16.93	-16.88	-16.90	-17.07	-15.89	-15.81	-16.28	-16.37	-16.16	-16.17
-1.20	-14.32	-14.42	-14.69	-14.83	-15.00	-13.60	-13.59	-14.17	-14.30	-14.31	-14.32
-1.10	-12.30	-12.59	-13.12	-13.42	-13.59	-11.54	-11.60	-12.35	-12.64	-13.02	-13.04
-1.00	-11.01	-11.43	-11.98	-12.41	-12.58	-9.69	-9.81	-10.78	-11.37	-12.06	-12.07
-0.90	-10.13	-10.75	-11.46	-11.83	-12.00	-8.21	-8.40	-9.84	-10.85	-11.31	-11.33
-0.80	-9.62	-10.33	-11.08	-11.40	-11.57	-7.72	-7.93	-9.56	-10.74	-11.06	-11.07
-0.70	-9.31	-9.95	-10.59	-11.01	-11.18	-8.23	-8.40	-9.28	-10.27	-10.96	-10.97
-0.60	-8.91	-9.42	-9.87	-11.31	-11.48	-9.72	-9.74	-8.78	-9.35	-10.24	-10.25
-0.50	-9.22	-9.33	-9.39	-9.41	-9.58	-11.69	-11.42	-9.18	-9.27	-9.46	-9.47
-0.40	-10.49	-9.91	-9.37	-9.40	-9.57	-14.24	-13.68	-11.35	-10.04	-9.84	-9.85
-0.30	-12.65	-11.56	-10.90	-10.42	-10.59	-16.51	-15.95	-13.32	-11.59	-10.87	-10.88
-0.20	-15.06	-13.48	-12.57	-11.94	-12.08	-19.05	-18.22	-15.70	-13.48	-12.31	-12.32
-0.10	-17.46	-15.49	-14.38	-13.48	-13.30	-21.62	-20.47	-17.73	-15.26	-14.07	-14.04
0.0	-19.84	-17.55	-16.19	-15.01	-14.48	-24.19	-22.73	-19.80	-17.07	-15.86	-15.77
0.10	-22.20	-19.61	-17.94	-16.52	-15.75	-26.74	-25.02	-21.92	-18.98	-17.53	-17.42
0.20	-24.56	-21.68	-19.66	-18.02	-17.05	-29.28	-27.32	-24.06	-20.94	-19.15	-19.02
0.30	-26.90	-23.76	-21.37	-19.52	-18.35	-31.83	-29.63	-26.21	-22.92	-20.77	-20.62
0.40	-29.24	-25.85	-23.07	-21.03	-19.67	-34.39	-31.95	-28.36	-24.88	-22.39	-22.22
0.50	-31.58	-27.94	-24.79	-22.56	-20.98	-36.99	-34.27	-30.50	-26.82	-24.04	-23.85
0.60	-33.90	-30.04	-26.51	-24.11	-22.30	-39.62	-36.62	-32.62	-28.73	-25.73	-25.51
0.70	-36.20	-32.16	-28.23	-25.68	-23.63	-42.23	-38.97	-34.74	-30.63	-27.44	-27.19
0.80	-38.50	-34.28	-29.95	-27.25	-24.96	-44.95	-41.33	-36.86	-32.51	-29.15	-28.86
0.90	-40.81	-36.38	-31.67	-28.83	-26.28	-47.53	-43.69	-38.99	-34.40	-30.86	-30.53
1.00	-43.15	-38.47	-33.40	-30.41	-27.58	-50.29	-46.05	-41.12	-36.28	-32.56	-32.18
1.10	-45.52	-40.53	-35.13	-31.98	-28.86	-52.94	-48.40	-43.26	-38.17	-34.24	-33.81
1.20	-47.91	-42.59	-36.86	-33.56	-30.13	-55.59	-50.75	-45.40	-40.06	-35.92	-35.42
1.30	-50.30	-44.63	-38.59	-35.14	-31.38	-58.25	-53.10	-47.55	-41.94	-37.59	-37.03
1.40	-52.71	-46.65	-40.33	-36.73	-32.63	-60.89	-55.46	-49.71	-43.83	-39.25	-38.62
1.50	-55.13	-48.68	-42.06	-38.32	-33.86	-63.54	-57.81	-51.86	-45.71	-40.91	-40.21
1.60	-57.56	-50.68	-43.80	-39.90	-35.08	-66.19	-60.16	-54.03	-47.59	-42.56	-41.78
(TJ/TO)	3.00	3.00	3.00	3.00	3.00	3.50	3.50	3.50	3.50	3.50	3.50
LOG(VJ/AO)	0.125	0.150	0.175	0.200	0.225	≤0.100	0.125	0.150	0.175	0.200	0.225

5.2 Flight Condition:

Forward speed has the effect of reducing shear velocities between the jet and its environment. Work in recent years has produced conflicting evidence on the change in jet mixing noise in going from static to flight conditions. Model scale wind tunnel testing has, in general, produced a greater reduction in level than tests carried out on ground based engine facilities and aircraft. The differences may be associated with contamination by other sources, both engine based and aircraft installation induced. The method herein is based upon data obtained on a ground based engine flight simulation facility, and in general the results fall between the extremes represented by some model tests and some aircraft flight tests.

The method relies upon a modification of the static sound pressure levels obtained in 5.1.

For a jet of given velocity V_j (corresponding to a given pressure ratio and temperature), moving at a flight speed V_a, the method of calculation is as follows:

Step 1 - Calculate the free field static overall sound pressure levels (OASPL) versus angle to inlet axis, as outlined in steps 1 to 4 of 5.1, corresponding to these exhaust conditions.

Step 2 - Calculate the OASPL in flight at any desired angle θ_i $(20° \leq \theta_i \leq 160°)$:

$$\left[\text{OASPL}\ (\theta_i)\right]_{\text{flight}} = \left[\text{OASPL}\ (\theta_i)\right]_{\text{static}} - \Delta\ \text{OASPL}\ (\theta_i)$$

where:

$$\Delta\ \text{OASPL}\ (\theta_i) = 10 \log_{10} \left[\left(\frac{V_j}{V_j - V_a} \right)^{m(\theta_i)} (1 - M_a \cos \phi) \right]$$

with:

$m\ (\theta_i)$ = relative velocity exponent, a function of angle θ_i between the engine inlet axis and the line connecting an aircraft reference point * and the observer location; $m\ (\theta_i)$ is given by Fig. A.12 and Table A.12

$M_a = V_a / a_o$ = Aircraft flight Mach number or ratio of airspeed V_a to speed of sound a_o at the desired ambient temperature of the surrounding medium.

ϕ = angle between direction of aircraft motion and direction of propagation (see sketch next page).

V_j = ideal fully expanded jet velocity, corresponding to a given pressure ratio and total temperature of the jet and being the same in static and in flight.

NOTE: For consistency with the prediction procedure under static conditions, this reference point * should be the center of the nozzle exit. For practical applications (aircraft noise predictions) alternative reference points may have to be selected (e.g. center of the engine nacelle, etc. . .).

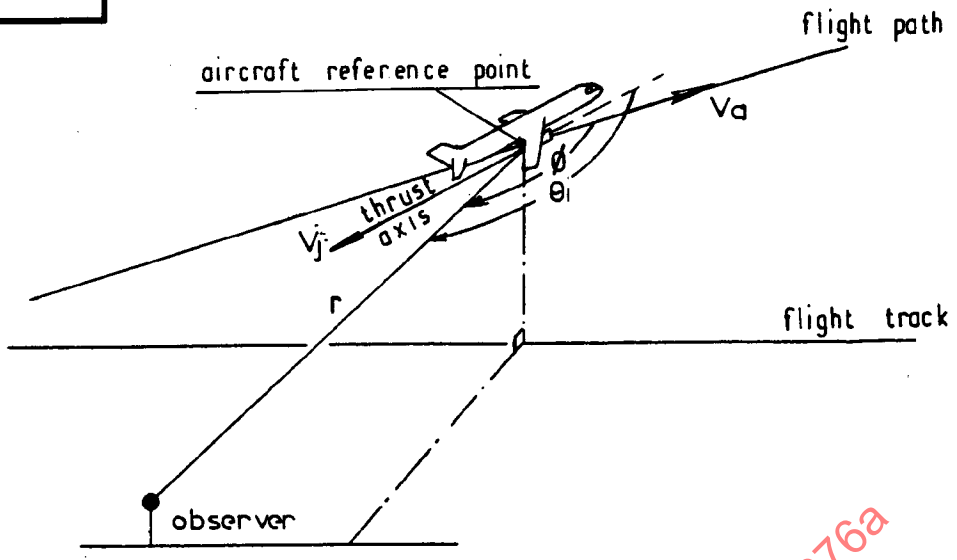

Step 3 – Calculate the one third octave band spectral levels in flight for any desired angle θ_i, following steps 5 and 6 of 5.1., with the exception that now the OASPL is the value in flight as derived in step 2 of this section and that the Strouhal number

ø

$$\left[\frac{f\,D_j}{V_j} \cdot \frac{1}{\xi}\right]$$

has to be replaced by one based on relative jet velocity $(V_j - V_a)$

$$\left[\frac{f\,D_j}{V_j - V_a} \cdot \frac{1}{\xi}\right]$$

The value of ξ is still obtained from Fig. A.3 for the corresponding value of the jet velocity V_j.

NOTE: Accuracy of Prediction

The accuracy of ΔOASPL (θ_i) prediction, as calculated in step 2 for any angle θ_i, is a function of velocity ratio, and may be obtained from the following formula:

$$\pm\,\delta\left[\Delta\text{OASPL}\,(\theta_i)\right] = \pm\left[\delta\ m\ (\theta_i)\right]\ \left\{10\log_{10}\left[V_j/(V_j - V_a)\right]\right\}$$

$\delta m\ (\theta_i)$ being the uncertainty in m (θ_i).

In the present prediction procedure, the range of uncertainty of the exponent m (θ_i) with respect to aircraft flight test data is estimated to be $\pm$one unit. This comment does not apply to wind tunnel model data where the exponent m (θ_i) is always greater over the angular range θ_i between 60° and 130° in the range 0 to 5 units.

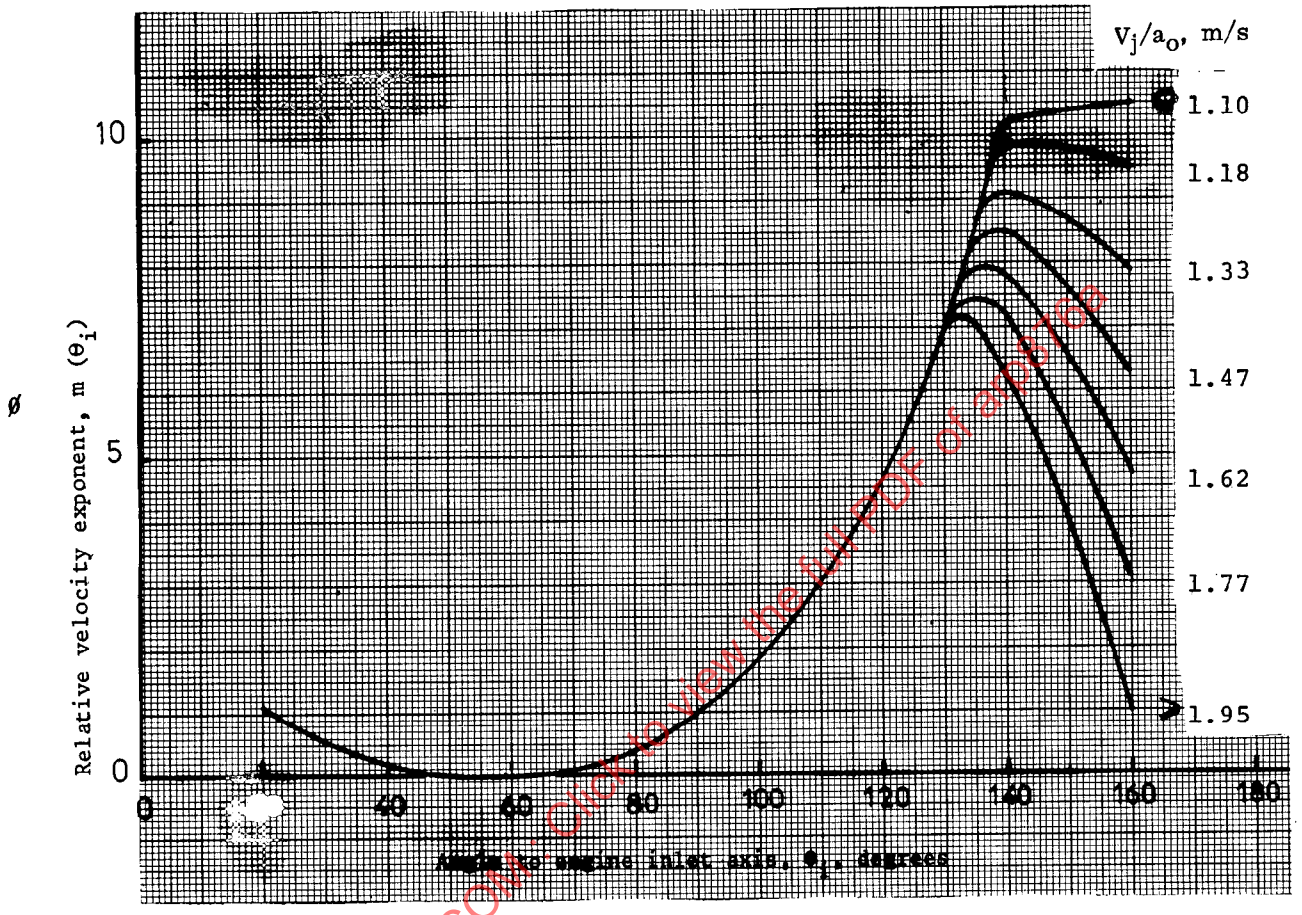

Figure A.12 Variation of velocity exponent m (θ_i) with angle θ_i and jet velocity V_j

θi degrees	m (θi)
20	1.1
30	0.5
40	0.2
50	0
60	0
70	0.1
80	0.4
90	1.0
100	1.9
110	3.0
120	4.7
130	7.0

ø

m(θi)

θi degrees \ V_j/a_o	≤1.10	1.18	1.33	1.47	1.62	1.77	≥1.95
140	10.2	9.8	9.1	8.5	7.8	7.2	6.3
150	10.4	9.8	8.7	7.6	6.5	5.4	4.0
160	10.5	9.5	7.9	6.3	4.7	3.1	1.0

Table A.12

Relative velocity exponent m (θ_i)

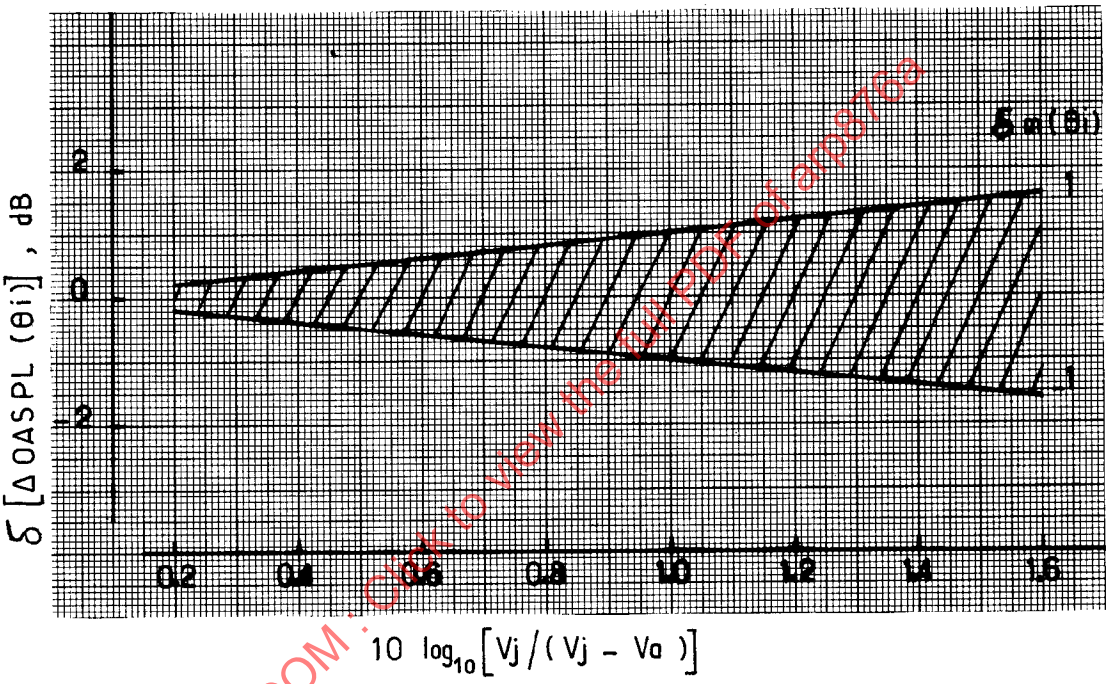

Figure A.13 Estimated range of uncertainty associated with calculated values of ΔOASPL (θ_i) for various jet velocity ratios and uncertainty in m (θ_i).

5.3 Parties Contributing to Formulation of Appendix:

Department of Transportation, USA
Douglas Aircraft Company, USA
General Electric, USA
Hamilton Standard, USA
Lockheed California Company, USA
Lockheed Georgia Company, USA
National Aero & Space Administration, USA
National Gas Turbine Establishment, United Kingdom
Pratt & Whitney Aircraft Company, USA
Rolls-Royce Limited, United Kingdom
SNECMA, France
The Boeing Company, USA

6. NOTES:

6.1 Marginal Indicia: The phi (Ø) symbol is used to indicate technical changes from the previous issue of this document.

APPENDIX B

DATE OF COMPILATION
March 1980

6. PREDICTION OF SINGLE STREAM SHOCK-ASSOCIATED NOISE FROM CONVERGENT NOZZLES AT SUPERCRITICAL CONDITIONS

6.1 Static Conditions: An incorrectly expanded supersonic jet contains shock waves which interact with jet turbulence to product a source of noise in addition to that due to the turbulent mixing process. While shock-associated noise may be reduced by attention to nozzle design, this source of noise is always present with a circular convergent nozzle. Allied to the theoretical approach of Ref. 1, definitive model and full scale experimental work (Refs. 2 and 3) has provided the following procedure for estimating the broadband shock-associated noise content. Taken together with the mixing noise prediction procedure of Appendix A, this enables the prediction of total noise from the shock containing under-expanded jet to be executed. The method provides for the estimation of the one-third octave band Sound Pressure Levels, which can be added by decibel summation to the levels obtained from Appendix A.

Shock waves in a choked jet are responsible for the source of broadband noise which is a function of pressure ratio and nozzle diameter. The method of estimation relies upon the derivation of the one-third octave Sound Pressure Level at any angle Θ_j and frequency f from the formula:

$$SPL\ (r, \Theta_j, f) = 10 \log_{10} \left[1 + \left(\frac{4}{Nb}\right) \sum_{i=1}^{N-1} \left\{ \left[C_1(\sigma)\right]^{i^2} \times \sum_{s=0}^{N-(i+1)} \left(\frac{1}{q_{is}^{\sigma}}\right) \left\{ \cos(q_{is}\sigma) \sin(bq_{is}\sigma/2) \right\} \right\} \right] + 10 \log_{10} \left[\left(\frac{D_j}{r}\right)^2 \beta^n \right] + 10 \log_{10} \left[b\sigma \right] + H_o(\sigma) + 148.8 \qquad (1)$$

where

$$q_{is} = \frac{1.70\, i}{(V_j/a_o)} \left[1 - 0.06 \left(s + \frac{i+1}{2} \right) \right] \left(1 - 0.7 \frac{V_j}{a_o} \cos\Theta_j \right) \qquad (2)$$

NOTE 1:

Symbols in Section 4 apply and,

$H_o(\sigma)$ = group source strength spectrum, dB)
$C_1(\sigma)$ = correlation coefficient spectrum) master spectra given in Fig. B1 and Table B1

N = 8 (number of shocks)

b = 0.2316 (for one-third octave proportional bandwidth)

$\omega_c = 2\pi f$